N O T I C E

THIS DOCUMENT HAS BEEN REPRODUCED FROM MICROFICHE. ALTHOUGH IT IS RECOGNIZED THAT CERTAIN PORTIONS ARE ILLEGIBLE, IT IS BEING RELEASED IN THE INTEREST OF MAKING AVAILABLE AS MUCH INFORMATION AS POSSIBLE

77N 27478

NASA TECHNICAL MEMORANDUM

NASA TM-76607

DEPOSITION OF THIN INSULATION LAYERS FROM THE GAS PHASE

Reinhard Behn, Horst Hagedorn, Johann Kammermaier, Manfred Kobale, Horst Packonik, Dietrich Ristow, Gerhard Seebacher

(NASA-TM-76607) DEPOSITION OF THIN INSULATION LAYERS FROM THE GAS PHASE (National Aeronautics and Space Administration) 86 p HC A05/MF A01 CSCL 07D

N82-14307

Unclas
G3/25 06249

Translation of "Abscheidung dünner Isolationsschichten aus der Gasphase", Siemens AG, Munich, Unternehmensbereich Bauelemente Hauptbereich Grundlagenentwicklung, and Bundesministerium fuer Forschung und Technologie, Munich, West Germany, Report BMFT-FB-T-76-66, May 1976, pp 1-88

NATIONAL AERONAUTICS AND SPACE ADMINISTRATION
WASHINGTON, DC 20546 JULY 1981

STANDARD TITLE PAGE

1. Report No. NASA TM-76607	2. Government Accession No.	3. Recipient's Catalog No.
4. Title and Subtitle: DEPOSITION OF THIN INSULATION LAYERS FROM THE GAS PHASE		5. Report Date JULY 1981 6. Performing Organization Code
7. Author(s) Reinhard Behn, Horst Hagedorn, Jchann Kammermaier, Manfred Kobale, Horst packonik, Dietrich Ristow, Gerhard Seebacher		8. Performing Organization Report No. 10. Work Unit No.
9. Performing Organization Name and Address SCITRAN Box 5456 Santa Barbara, CA 93108		11. Contract or Grant No. NASw-3198 13. Type of Report and Period Covered Translation
12. Sponsoring Agency Name and Address National Aeronautics and Space Administration Washington, D.C. 20546		14. Sponsoring Agency Code

15. Supplementary Notes: Translation of "Absheidung dünner Isolationsschichten aus der Gasphase", Siemens AG, Münich, Unternehmensbereich Bauelemente Hauptbereich Grundlagenentwicklung, and Bundesministerium fuer Forschung und Technologie, Munich, West Germany, Repopt BMFT-FB-T-76-66, May 1976, pp 1-88 (Original German: N77-29418)

16. Abstract: By glow discharge in monomer gases organic dielectric films (with a thickness down to 100 nm) could be deposited on metallized carrier foils in a continuous process. Depending on the applied monomers, the films had a dissipation factor of 1×10^{-3} to 3×10^{-3} (1 kHz), a relative permittivity of 2.3 to 2.5 and a resistivity of about 10^{17} Ωcm. Additionally, they proved to have a very mechanical homogeneity. Self-healing rolled capacitors with a very high capacitance per volume and of consistantly high quality (68 $\mu F/cm^3$) were fabricated from the metallized carrier foils covered with the dielectric film deposited there on.

17. Key Words (Selected by Author(s))	18. Distribution Statement: Unclassified - Unlimited		
19. Security Classif. (of this report) Unclassified	20. Security Classif. (of this page) Unclassified	21. No. of Pages 86	22. Price

Federal Ministry for Research and Technology

Research Report T 76-66
Technological Research and Development
- Electronics -

Deposition of Thin Insulation Layers from the Gas Phase

Siemens AG, Munich
Unternehmungsbereich Bauelemente
Hauptbereich Grundlagenentwicklung

Munich, May 1976

Department leader:
Dr. Hermann Heywang

Project direction:
Reinhard Behn

Preparers:
Reinhard Behn
Horst Hagedorn
Dr. Johann Kammermaier
Dr. Manfred Kobale
Horst Packonik
Dr. Dietrich Ristow
Dr. Gerhard Seebacher
et al.

Table of Contents

* Numbers in margin indicate pagination of original foreign text

1 INTRODUCTION /8

The "Deposition of thin insulation layers from the gas-phase" is the promoted part of a larger endeavor which has as its goal the development of capacitors with plastic dielectric for high energy density. Capacitors with plastic foils such as polystyrole, polyethyleneterephthalate, tradename "Hostaphan" (Hoechst) or "Mylar" (Du Pont) and polycarbonate, tradename "Makrofol" (Bayer) receive a great technological and economic significance because of their high dielectric strength, their low water take-up and the potential to produce thin foil thicknesses. Because of these properties the dimensions of plastic capacitors could constantly be reduced and the energy densities could be increased considerably. However, limitations, till now insurmountable, were set for the possibilities for applying ever thinner foils by the increasing difficulties during the processing, e.g., during winding and metallizing. Thus the producers of foil, after initial rapid progress, which led to a thickness of 2 μm, were unable in the last few years to achieve additional success with respect to thinner foils.

Even before 1960 Siemens developed a method by which the dielectric layers could be produced from a fabrication-technological standpoint down to 1.2 μm and which led to the well-known MKL capacitor. Here the dielectric medium is applied to the carrier foil in the form of a lacquer, is metallized, and subsequently again removed from the capacitor from the carrier foil during the winding of the capacitor.

With the goal to find newer ways for producing even thinner dielectric layers with high dielectric strength for capacitors with high energy densities, we first investigated various methods from an orientation standpoint: the production of thinner layers by glow polymerization from the gas phase, the deposition of pyrolytically produced gases and finally layers from radiation polymerized material. /9

From this initial work it became apparent that the glow polymerization method from the gas phase for production of very thin dielectric layers showed the greatest promise for success. These developments were then continued forcibly with the support of the BMFT. With this method it now became possible to produce thicknesses down to 0.1 µm in large surfaces and to produce, despite the low thicknesses, very uniform, high-performance layers from an electric standpoint.

It was possible to base the development on extensive preliminary investigations which the receiver of the grant had already done as a preliminary performance. The starting point of this work was the status as of that time of the technology: basic investigations concerning the polymerizing capabilities of organic substances by means of glow discharges had already been made in 1931 by Linder and Davis /1/. Haefer and Mohamed /2/ and Carchano /3/ determined in detail the characteristics of the glow discharges and the behavior of ion and electrons in a D.C. field. According to them the affected cross-section of the cations for polymerization processes is greater than that of the electrons by an order of magnitude. Bradley and Hammes /4/ investigated the temperature dependence resistance of the layers produced by means of glow discharges in an HF-alternating field and determined the yield (g/kWh). Stuart /5/ presented a simple apparatus for flow-through coating of aluminum foil. Connell and Gregor /6/ utilized a longitudinal magnetic field for generating an electrode-free glow discharge in order to obtain layers as pure as possible without imbrittlement, such as can happen during direct ion bombardment. A great number of investigations were concerned with the property of certain polymerides /7-11/. Mostly two plate- /10
shaped electrodes were used which are contained in an evacuated receiver, which is being flooded through with the gas to be polymerized up to a definite pressure. Here the plates serve also as carriers for the polymer layer. At times the work done in the references cited was performed in a stationary system, i.e., after filling the receiver with the appropriate starting monomers

to a working pressure without additional gas supply and without pumping, partly with a dynamic equilibrium where fresh gas was constantly supplied and where gas enriched with products of cracking was pumped away.

In view of the state of the technology it was necessary to develop an apparatus which allows a very uniform and very thin deposition of a metal-like carrier foil in a flowing system. A metallized carrier foil became necessary, because the prerequisite for applying these thin glow polymer layers as dielectrics in capacitors are a self-healing capacitor construction. In addition it was necessary to develop new dielectric materials with improved properties whose chemical composition also satisfies the requirements for self healing in capacitors.

The following sequence was provided for planning the work: first it was intended , building on the experiences with a simple already available apparatus , to build a new installation in order to assure a disturbance-free coating process in order to improve the quality of the coating. Simultaneously it was needed to conduct an investigation of the layers produced with respect to insulation behavior and further dielectric properties. With a view to a later economic application of this process we aimed at an increase in the deposition speed of the layer. The chemical structure of the layers obtained had to be determined whereby infrared spectroscopic investigations had to be conducted. The investigation of the adhesive property of the layers on one another (carrier foil, metal vapor deposition and glow polymerization deposition) was also an important work item. Finally it was intended to produce capacitors from the thin dielectric layers and to investigate their properties in short- and long time tests.

It was possible to conduct the work sequence in accordance with a plan stipulated in the contract with one small authorized change which also included the investigation of the self-healing properties of these thin layers.

During the conduct of the FE-project the receiver of the grant was not aware of any additional progress made in this area and other places.

2. Construction of the coating apparatus

2.1 Introduction

With the help of a glow discharge it was possible to polymerize organic gases and vapors /12/. Here the molecules in the discharge path were broken up into radicals and ionized by the breakup of covalence bonds and/or by separation of gaseous components (H-atom, methyl groups and similar). In the boundary regions of the discharge region the radicals recombined to larger complexes by mutual saturation of their valences. This process proceeds preferably at the electrodes of the discharge path, the precipitated particles combine to macromolecules and form adhesive layers. By means of glow discharge it is also possible to excite, for the formation of macromolecules, materials which cannot be polymerized by conventional chemical methods. Not only is it possible to separate active groups, such as substitutable H-Atoms, /12
methyl groups and multiple bondings, but also more stable bondings such as H-atoms from benzene rings. The elementary processes in the glow discharge and during polymerization are not yet known.

Only a certain pressure range of glow discharge is suitable for polymerization. The arc discharges occurring at atmospheric pressure cannot be used for coat formation because of the extraordinarily high current densities. Only for pressures in the range

of about 1 mbar does the current density become so small that it does not affect electrodes- and carrier material and the properties of the coating. Investigations with a simple test apparatus, such as is being used in the work referred to at the beginning, now demonstrated the exact conditions under which the formation of the coating is possible. The results will be described in the following.

2.2 Results of the preliminary tests

The partial pressure p of the reaction gases must be in the range of 1...6 mbar. For higher pressure the discharge became non-uniform, the resulting polymerization layer exhibited variations in thickness and murky appearance and its dielectric losses increased. For pressures that were too low the dielectric losses also increased since a certain partial pressure of impurities - especially oxygen which as a reactive element takes part in the polymerization process - could not be avoided in the reacting chamber so that, as the partial pressure of the monomers was reduced, the relative portion of the impurities increased. This led to an increased introduction of impurities into the polymer layer. With a knowledge of the optimal pressure we obtained, according to Paschen's Law for the arc voltage $U = f(p \cdot d)$ also the optimal electrode distance of $d \approx 12$ mm. The optimum current density was found to be 0.2... 5 mA per cm^2 electrode surface. For a current density that was too low the discharge burned non-uniformly, i.e., it extended only to a part of the electrode surface. For too great a current density the temperature gradient between layer surface and electrode became too great so that, because of stresses, the layer exhibited cracks and/or lifted from the substrate. Therefore, the temperature measured at the electrode back side must not exceed $150^{\circ}C$.

2.3 Construction of the new apparatus

2.3.1 Roller-guidance system and electrode arrangement

In accordance with the knowledge gained a new apparatus was constructed which permits coating in a flowing system. It is described in the following.

The new apparatus is placed in a 50 liter vacuum chamber (figure 1). It consists of a moving roller system and three electrode pairs in parallel facing each other. A carrier foil (carrier for the polymerization layer) coming from a supply roll is pulled across the two-dimensional surface in such a way that it just touches it. Subsequently, it is again wound onto another roll. The excitation frequency of the glow discharge was increased by means of a power sender (minimum power 200 W) to 100 kHz...1 MHz so that the displacement current through the carrier foil is sufficient to maintain the glow discharge. Since for one electrode pair on each of the surfaces facing each other polymerization layers are deposited, one carrier foil is simultaneously pulled through for each surface so that two supply rollers and two takeup rollers are installed. The width of the carrier foil is the same as the width of the electrode surface so that the electrodes are protected from the discharge zone. In this way the electrodes remain clean and even longer test foils can be coded in one run. Since the dimensions of a flat electrode pair are limited by the danger of wrinkle formations in the carrier foil, we resorted to several /14
parallel-connected electrode pairs whereby a foil between the electrode pairs was smoothened by means of reverse direction rollers. This also has the advantage that the carrier foil, during the coating process, can cool off on the reverse direction rollers outside of the glow discharge volume. The area of the electrodes is 150 x 100 mm^2 each. So that no electrical discharges can occur at the electrode edges which could damage the carrier foil, the edges are coated with

an insulating strip made of teflon. To reduce the thermal loading of the carrier foil the electrodes are water cooled. We were able to dispense with the originally used oil cooling with heat exchanger because water, at the presently used high excitation frequencies, has a sufficient insulation resistance with respect to the electrodes.

The installation is layed out for foil width up to 150 mm and should wind carrier foil thicknesses down to 2...3 µm without any problems. It turned out that disturbing electrical field effects arose at the mounting place for the roller system and that even discharges originated from the electrodes which forced us to make the carrier plates out of plastic. For reasons of mechanical stability and accuracy, bearings had to be installed on both sides of the rollers when using the plastic structure. After testing of several plastics epoxy resin proved to be the best. The electrode pairs are also mounted on these plastic plates. The distance between the electrode pairs between which the glow discharge takes place can be changed rather simply. The electrode supports are constructed in such a way that, by means of adjusting screws, the position and tilt of the electrodes can be adjusted exactly parallel to the path of the foil. Thus it is possible, despite the relatively large electrode surfaces, to move the carrier foil without displacement and without the formation of wrinkles.

2.3.2 Measures for stabilizing the glow discharge

Tests showed that now and then discharges occurred through the foil exposed to the glow up to the electrode. Therefore, the discharge surfaces of the electrodes facing each other are covered with an insulation layer of several micron thickness which serves for stabilizing the discharge. This insulation layer prevents current concentration resulting from discharge. The electrical substitute circuit diagram, shown in figure 2 /13/, corresponds to the given buildup between the electrodes.

We have: $\frac{1}{\omega C_g} \gg R_g$ and $R_s \gg \frac{1}{\omega C_s}$ (ω = angular frequency of generator

C_g = capacitance of glow volume, R_g = resistance of glow volume

C_s = capacitance of insulating layer, R_s = resistance of insulating layer)

To a good approximation the resistance of the entire arrangement thus is

$$|Z| = \sqrt{\frac{4}{\omega^2 C_s^2} - R_g^2}$$

For the glow discharge a voltage U_{eff} between 200 to 400 V was required if the gases described below were used and if an experimentally determined current density flowed which was optimal with respect to polymerization speed and thermal stresses of the carrier material. From this we obtained, according to the schematic arrangement in figure 2, a resistance in the glow discharge volume of 100,000 to 200,000 ohms, referenced to an electrode area of 1 cm^2. Then in the insulating layer on the electrodes the voltage decreased by U_s.

$$U_s = \frac{d \cdot I}{\omega \cdot \varepsilon \cdot \varepsilon_0} \qquad (1b)$$

(d = thickness of the insulation layer, I = current density,
ε = dielectric constant of the insulating material)

For sufficiently high frequency of the discharge current the voltage drop U_s was less than 1 V. /16

The formula (1b) also applies for the voltage drop at the carrier foils located in the glow region.

In addition to these measures the metal coat of the plastic foils to be coated was set via an electrically conducting reversing roller at the potential of the associated electrode.

For disturbance-free glow the required energy is transported to an overwhelming degree by the displacement current through the insulation layers into the glow zone.

2.3.3 Drive system

A 400 W D.C. motor, located outside of the reaction chamber and controlled by a thyristor switch, provided the drive of which high requirements were made with respect to synchronism. The torque is transmitted to the wind-up rollers via a chain drive, a rotary feed-through for the vacuum system, and a system of gears.

For thermally sensitive carrier foils it was not possible to apply arbitrarily thick glow polymerization layers in one work step since the heat loads resulting from the heat of reaction and from the current flow would have led to partial destruction of the carrier foil. Therefore, thick layers were produced in several work runs. Tests were also conducted to coat various dielectrics at very small thicknesses (10 ... 100 nm) directly on top of one another in order to achieve certain defined properties of the dielectric layers which cannot be achieved with a one-material system.

To avoid intermediate aeration with corresponding adsorption of air and water, it was necessary to find a way by which the carrier foils could be rewound in the reaction vessel. Because of the changes in diameter between the supply- and wind-up rollers no common rigid drive could be used for both rollers. It had to be possible to decouple the roller to be unwound. A solution for the drive principle was found through magnetic couplings so that it was now possible to wind and unwind the carrier foils at random without opening the reaction vessel. /1

For coating thicknesses of 50 to 150 nm running speeds of the order of 1 m/min are required. With this apparatus running speeds of 0.1 m/min to 10 m/min are possible.

2.3.4 Direct gas supply

For electrode surfaces of dimensions 150 mm x 100 mm inhomogeneities arose in the glow discharge volume, recognizable by non-uniform glows of the discharge, which became noticeable by uneven thicknesses and by an insufficient quality of the polymer layer. As tests showed, this phenomenon can be attributed to a lack of fresh-gas supply and too high a concentration of cracked products in the interior region of the discharge volume.

For that reason an attempt was made to pass the fresh gas directly into the discharge volume. As a first step we used a carrier foil which we led over the associated electrode plate. The opposite electrode consisted, at the side facing the discharge region, of porous sintered bronze with pores of 100 µm diameter through which the fresh gas flowed into the discharge volume. The pores could not be closed by polymer deposits resulting from the flowing gas (figure 3).

In a subsequent step it became possible to utilize both electrode pairs, i.e., to coat 2 foils at the same time. Here insulating cover strips were used for gas supply which limit the discharge volume during entry resp. leaving of the foil from the glow zone and which cover the reversing roller system. The strips were hollow and were provided with a row of holes (1 mm diameter) /18
leading to the discharge volume. In this way the fresh gas could be passed directly into the discharge volume. The coatings produced with this gas supply system are unobjectionable under full utilization of the capacity of the installation.

For the continuous supply of the installation with monomer gas, a flow-control valve was installed between the supply container and the reaction vessel. Simultaneously with gas admission of gas the vessel was pumped down to a limited extent since, during the

glow process, cracked products (hydrogen, methyl groups, and similar) were produced which could have a damaging effect on the quality of the layer if present in too high a concentration. With the aid of the flow-control valve the partial pressure of the monomer had to be kept constant to ± 10% of the monomer-dependent rated value (between 100 and 700 N/m^2) in order to achieve a uniform polymerization speed.

With all these measures it became possible to produce coat thicknesses down to 0.1 µm with great uniformity of thickness (± 2.5%) and with homogeneous quality.

3. The investigation of the insulation resistance, the dielectric properties, and of self-healing

3.1 Introduction

For application as capacitor dielectrics the insulating action, the dielectric properties, and the self-healing of these thin layers is of decisive significance. For coat thicknesses of about 0.1 µm very high field strengths are obtained in the dielectric (200 V/µm) even for low capacitor voltages (e.g., 20 V). The investigation of the layers thus not only penetrates new areas from the standpoint of new materials, but also the operating field strengths attain values which are not yet being used in general in dielectrics known today.

As is known from investigations with plastic foils /14/, the insulation current increases, in the region of higher field strengths, to an increasing degree with increases in voltage. The magnitude of the insulation currents and its dependence on temperature, time, and field strength therefore affects the type and thickness of the dielectric for a given applied voltage. /19

Even a knowledge of the dielectric properties of the layers, such as dielectric constant and loss factor, is very important in its application in capacitors.

Self-healing has not yet been investigated for layers of this thickness. Since these low layer thicknesses cannot be produced without voids (e.g., pores), we must assume that self-healing takes place so that the capacitors attain high dielectric strength and high insulation. For self-healing a certain energy is required for vaporizing the electrode metal at the arcing location. In general only the energy stored in the capacitor is available for that. For the presently used thin layers with their relatively low arc voltages, this question is worthy of further investigation.

3.2 Investigation of the insulation resistance

3.2.1 Experimental conduct

In figure 4 the principal construction is shown for those capacitor models with which the investigation of the dielectric properties of the glow polymer layers was conducted. A metal coating - primarily aluminum - was applied to relatively thick plastic foils, especially polyethylene terephthalate, by a vapor deposition process in high vacuum. Upon this metallized carrier foil we find the glow polymer layer and upon it the vapor-deposited counter-electrode. It proved to be advantageous for most of the investigations to use small-area model capacitors with capacitance-effective areas in the range 0.5 cm^2 to 1 cm^2. For higher capacity condensers longer strips of the above-mentioned construction with capacitance-active areas between 100 and 1000 cm^2 were wound and contacted. In addition to aluminum, other metals were occasionally used, such as copper, zinc, or mercury, as electrode metals for at least one of the two electrodes. /20

During the measurement the samples were placed in a vacuum oven which, at the same time, produced shielding and in which the samples were tested with the assurance of good drying at a pressure of 2 mbar and at temperatures in the range of 20° C ... 120° C. For comparison measurements were also made with undried samples.

To determine the at times rather small currents, an oscillating condenser electrometer made by the Keithley Instruments Co. of type 640 A proved to be especially suitable. The instrument makes possible current measurements down to 10^{-17} A for practically no zero drift (input resistance optional to above 10^{16} ohms. input capacitance < 2pF).

For measurement of the current-voltage characteristic lines of the insulation layers high demands are made of the D.C. supply. For the measurements an instrument, stabilized electronically to 10^{-4} for $\pm$ 10% network voltage fluctuations, was employed.

For application of polymerized coatings in high-performance dielectric capacitors, starting monomers with the gross formula $(CH_2)_n$ and $(CF_2)_n$ produced at a minimum vapor pressure of $3 \cdot 10^3$ N/m^2 turned out to be particularly suitable.

For investigating the insulation properties we selected from the two groups of materials, cyclohexane with the gross formula C_6H_{12} and perfluorocyclobutane (gross formula C_4F_8) as characteristic materials.

Most of the samples produced first were subject to short-circuits which, however, could be eliminated by directed voltage loads (called unlocking).

3.2.2 Measurement current density, results, and their discussion /2

The current density was determined with capacitor models with a glow polymer dielectric made of cyclohexane (figure 5) respectively perfluorocyclobutane (figure 6) and layer thicknesses of 100 nm. In order to eliminate post-charge events during the insulation measurement, the current density values were not read off until 60 minutes after the measurement voltage had been applied to the model capacitor.

Now and then self-healing took place because of the long duration of the measurement and the relatively high field strength. Measurements for which a self-healing process was observed, recognizable by a short current jump could not be evaluated for determining the insulation resistance.

When the 60-minute values of the insulation currents are plotted, one obtains as a good approximation straight lines if $\sqrt{U}$ (U = measurement voltage for the materials tested) is chosen as the abscissa (figures 5 and 6). Even for the well-known plastic foils for capacitors, such as polyethylene terephthalate, analogous insulation measurements lead to straight lines according to figures 5 and 6. In figure 7 the current density values are plotted as a function of field strength for 6 µm thick polyethylene terphthalate foils and for 100 nm thick glow polymer coatings made of hydrocarbons resp. of perfluorinated monomers as starting materials. In the following several values will be presented for the specific resistances: layers of cyclohexane for a field strength of 10 V/µm $5 \cdot 10^{18}$ Ωcm (25°C) or $2 \cdot 10^{16}$ Ωcm (100°C), for layers of hexafluoropropylene $1.6 \cdot 10^{17}$ Ωcm (25°C) or $1.6 \cdot 10^{15}$ Ωcm (100°C). The comparison values for a 6 µm thick foil of polyethylene terephthalate are : $2.5 \cdot 10^{18}$ Ωcm (25°C) or $1.6 \cdot 10^{15}$ Ωcm (100°C).

The conduction processes in these thin layers, which agree with the results from well-known plastic foils, are largely unknown. The evaluation of the test results showed that the relation between current density j, field strength E, and temperature T can be explained neither by the well-known Schottky equation /15/

$$j = AT^2 \exp\left(-\frac{\varphi_S}{kT} - \frac{BE^{1/2}}{T}\right)$$

with $A = 4\pi e m k^2/h^3$

$B = e^{3/2}/k\,(4\pi\varepsilon\varepsilon_0)^{1/2}$

φ_S = work function

e = elementary charge, m = mass of electrons

h = action quantum

nor by the Poole-Frenkel equation /16/

$$j = e\,b\,n\,E \exp\left(-\frac{\varphi_{PF}}{kT} - \frac{BE^{1/2}}{T}\right)$$

b = movability of the charge carriers

n = charge carrier density

φ_{PF} = excitation potential from disturbance locations in the conductive band

$$B' = 2\,e^{3/2}/k\,(4\pi\varepsilon\varepsilon_0)^{1/2}$$

The following was found for the relation between current density, temperature, and field strength for the glow polymerization layers in agreement with results obtained with plastic foils:

$$j = C \cdot \exp\left(-\frac{\varphi}{kT} - \frac{BE^{1/2}}{T}\right)$$

For glow polymer layers from cyclohexane the constant C has the value $8 \cdot 10^{-4}$ A/cm^2 and for perfluorinated glow polymer layers $1.8 \cdot 10^{-3}$ A/cm^2.

The term D, in contrast to the corresponding term in equations (1) according to Schotky and (2) according to Poole-Frenkel is temperature-dependent (see table 2).

φ_S denotes in (1) the work function for electrons exiting from electrode metals into vacuum (e.g., 2.8 eV for aluminum). From figures 5 and 6, for the corresponding term ϕ in (3), values between 0.6 and 0.7 can be calculated. For plastic foils such as polyethylene terephthalate values between 0.8 and 1.2 eV are listed /17/. /2

The just described deviations of the experimental results from the laws demanded by Schottky, especially the value of ϕ = 0.6 to 0.7 as determined by us compared to the much higher values φ_S for the work function of metals, suggest that the conducting electrons reach the conducting band not from the electrodes, but from disturbance places in the insulating layer. This is also in agreement with the fact established by us that the current density is independent not only of the electrode material, but also of the polarity of the voltage.

The constant B in formula (2) corresponds to that from (1) except for the factor 2. In table 1 the values for B, calculated according to Schottky with ε = 2.5 and according to Poole-Frenkel also with ε = 2.5, are compared with the quantity D from equation (3). One can clearly recognize the temperature dependency of D; furthermore it can be seen that the value D agrees with the value B calculated according to Schottky only at 25° C.

Table 1 Listing of the quantity B or D ($V^{-\frac{1}{2}}cm^{\frac{1}{2}}K$) from the formulas (1), (2), and (3)

	25°C	100°C
D for layers made of cyclohexane (d=100 nm)	1.54	1.83
D for fluorinated layers (d=100 nm)	2.53	3.00
D for polyethylene terephthalate (d=6 μm)	2.45	4.04
B calculated according to Schottky (with ε =2.5)	2.73	2.73
B calculated according to Poole-Frenkel (with ε = 2.5)	5.46	5.46

The comparison of formula (3) with that of (1) and (2) also shows that the conducting mechanism in thin layers deviates from that calculated according to Schottky as well as that according to Poole-Frenkel.

3.3 Dielectric properties /24

3.3.1 Dielectric constant and losses

The investigation of the current density was complemented by additional measurements of capacitance and of losses. It was also conducted with capacitor models according to figure 4. To achieve dielectric properties as good as possible we first selected materials which, in chemical polymerization, produced non-polar materials such as polyethylene or tetrafluoroethylene. As the following dielectric investigations show only amorphous layers with more or less built-in dipoles can be produced by the creation of side chains and networks by means of glow polymerization not only for hydrocarbons but also for perfluorinated starting monomers. As a further step we then chose cyclic starting monomers with outside chains which break up on their end in the discharge zone of the glow polymerization apparatus to linear molecules with one free valence each and which then assemble to long chains with few side chains. As shown in table 2 even these layers were not free from dipoles, and an increase of the dielectric constant and the losses compared to chemically polymerized comparison materials was found.

The DZ-values listed in table 2 for glow polymer layers are obtained from capacitance measurements with capacitor models. The determination of the dielectric constant, accurate for the first time, was made by means of two methods: in one very plain silver mirrors were coated partially. With the interference microscope one was then able to determine the thickness of the

applied layer at the boundary between coated and uncoated carrier parts. By vapor deposition of a surface (F = 2 cm^2) defined as counter electrode the capacitance was measured and from that DZ was calculated. In the second method the coating thickness on plastic carrier foils was determined by weighing and by capacitance measurement. In order to obtain a weight ratio of the carrier to the coating as favorable as possible we selected 3 µm thick carrier foils. Metalized foil pieces of defined size (dimensions of the electrodes) were weighed. Subsequently they were coated and weighed again. After vapor deposition of counter electrodes of surface 2 cm^2 and capacitance measurements it was possible to calculate, in conjunction with the first method, layer thickness, specific weights, and DZ. By frequent repetition of these processes we obtained statistically assured results accurate to about ± 5%. Now it was possible to determine, in reverse direction, the thickness of glow polymer layers by capacitance measurements. /2

Table 2 DZ and tan δ of polyethylene and polytetraflurorethylene and the corresponding glow polymerides

	polyethylene	glow polymeride from cyclohexane	polytetrafluoroethylene	glow polymeride from perfluorcyclobutane
DZ (25° C)	2.3	2.5	2.1	2.3
DZ (100°C+)	2.25	2.55	2.04	2.26
tanδ · 10^3(25°C)	0.2	4	0.2	1.5
tanδ · 10^3(100°C)	0.2	5	0.2	1.5

+) The numbers were calculated from capacitance changes compared to the value at 25° C.

As a result of the insertion of dipoles we obtained change in the temperature dependency of the capacitance as compared to chemically polymerized plastic. While for nonpolar materials, such as polyethylene resp. polytetrafluoroethylene, with pure displacement polarization (because of the change in density with temperature) the DZ decreases with increasing temperature and a value for TK_c of about $-210 \cdot 10^{-6}.^{\circ}C$ is found, glow polymerized layers with cyclohexane as starting monomer exhibit a positive temperature value of capacitance with a value TK_c of about $+300 \cdot 10^{-6}/^{\circ}C$ (figure 8). An increase of DZ results from the fact /26
that the built-in dipoles become mobile at higher temperatures. Perfluorinated glow polymer layers with fewer numbers of built-in dipoles as compared to polyolefins exhibit at temperatures above 25° C a negative, but at lower temperatures a positive TK_c (figure 9).

The capacitance- and loss factor curves of the glow polymer layers are - as can be recognized particularly for those with cyclohexane as a starting monomer - relatively uniform without sharp extremes over the entire frequency - as well as temperature range that was measured. Accordingly there seems to be a smear or a wide interval of the thermal activation energies for excitation of dipole movement of the glow polymeride, which suggests a large number of polar structures.

3.3.2 Electrical arcing resistance

While for capacitors with metal foils the first arcing leads to short-circuits, arcing is basically allowed for self-healing capacitors. However, even here the number of arcings must be kept as low as possible during operation. Thus the question arises how the frequency of arcing depends on the various test parameters, such as voltage and temperature. A comparable measure for the arcing behavior of self-healing capacitors is obtained by a test, in which, for step-wise voltage increases of capacitors, the number of self-healing arcings is measured per voltage step.

In this way one obtains an idea of the number of arcings with reference to a given voltage and temperature. Since the number of arcings is approximately proportional to the decrease in capacitance, one can also choose in these tests the decrease in capacitance as a measure of the arcing resistance. Such tests are described in the following: They were conducted with capacitance - effective surfaces of 1 to 100 cm^2 and with dielectric thicknesses of 75 nm, 100 nm, and 150 nm. The results are shown in figure 10 where the rest capacity of the capacitors investigated is given as a function of the applied field strength. Up to a field strength of about 300 V/µm no arcing was determined. For higher loads the capacitance of the model capacitors decreased because of self-healing arcings. It was shown that the important capacitance decrease occurred in a relatively narrow range of field strength (Δ E = 100 to 150 V/µm). In figure 10 it can be recognized clearly that the arcing field strength increases with decreasing coat thickness. Such a behavior was described theoretically by Fröhlich /18/ and was confirmed by measurements of, however, very small area single crystals. To explain the thickness dependencies of the arcing resistance one can use the concept that the formation of electron avalanches necessary for generating arcings is made increasingly more difficult with decreasing coat thicknesses. /2

For industrial foils, such as polycarbonate or polyethylene-terephthalate the number of arcings per unit area, referenced to equal field strength, increases in the direction of thin foils /19/. The reason can be found in technically caused voids which, in thinner foils, are always more closely spaced. The tests with glow polymerides now show, in contrast thereto, an increase in arcing resistance as the layer thicknesses become thinner. In addition the arcings are all found in a relatively narrow field strength interval (at 150 nm: 450...550 V/µm, at 100 nm: 600...700 V/µm, at 75 nm: 750...890 V/µm). This behavior suggests an extraordinarily great homogeneity of the layers generated by glow polymerization.

The extremely high arcing resistances of these thin layers which at 75 nm have an average value of about 800 V/µm, suggest the question as to whether we're dealing here with intrinsic field strength. To visualize this let us remark that for this field strength 60 V lie at 200 molecule position (75 nm). Measurements are known with pure samples from polyethylene /20/ in the thickness range of 5 to 200 µm, for which, independent of thickness, an intrinsic field strength of 800 V/µm was measured. However, if this value is also valid for thickness values below 1 µm and whether the material properties enter here, is still unknown. Therefore, nothing can be said concerning the material-related arcing resistance of these glow polymer layers. /28

3.4 Investigation of self-healing

3.4.1 Test construction

The tests were conducted with models as shown in figure 4 (carrier foil 50 µm-polyethylene terephthalate, 150 nm and 300 nm thick, glow polymerized fluoro-carbon-dielectric). The capacitance effective electrode area had dimensions of about 1 mm x 8 mm; this produced capacitance value of about 2 nF resp. 1 nF. The one layer construction of the model made possible the direct observation of the arcing position.

During the test the voltage at the capacitor models was increased long enough until regenerative arcing took place. The voltage was increased slowly enough so that arcing took place at sufficiently long time intervals so that they could be observed individually. The changes in voltage were recorded with an electron beam oscillograph.

In order to be able to record the slow voltage increase as well as the sudden voltage decay resulting from arcing, the new voltage rise had to be delayed long enough so that it produced a visible

trace in the oscillogram. This was accomplished by the construction consisting of three RC-members shown in figure 11. A simple serious resistance at the test unit would have to be, because of it small capacitance, larger than 1 G Ω , which is difficult to achieve and which, because of the voltage division resulting from the internal resistance of the measuring instruments, produces problems in the voltage supply (compare also figure 14 and the associated text). The first RC-member (R_1C_1) had a time constant of about 10 s and served for the slow charging of the test unit C_{pr}. Because of the substantially smaller time constant of the two RC-members connected downstream the voltage at the capacitors C_2 and C_{pr} is equal during the charging phase. During arcing the voltage at the test unit decreases by ΔU (figure 12). Arcing is completed within one microsecond. During this time no significant amount of charge flows to the test unit through the resistor R_3. After that, however, the test unit is charged again within a few milliseconds from the capacitant C_2 until C_2 and C_{pr} have the same voltage. This produces a voltage decrease $\Delta U'$ (figure 12) at C_2 which is recorded by the measuring instruments. Then follows the slower recharging of C_2 and C_{pr} to the arcing voltage. /29

For the charging of C_{pr} from C_2 we have

$$(1) \quad C_2 \Delta U' = C_{pr} (\Delta U - \Delta U').$$

Therefore ΔU can be calculated simply from the measured $\Delta U'$.

$$(2) \quad \Delta U = (1 + \frac{C_2}{C_{pr}}) \Delta U'$$

This means that the scale factor of the oscillograph must be multiplied by the value in the parentheses in order to be able to read off ΔU directly. (The measuring errors during the determination of C_2 and C_{pr} can be neglected compared to the accuracy of reading the oscillograph).

3.4.2 Test results

By means of the described construction the arcing voltage U and voltage decrease $\Delta U = U_0$ was measured and from that the energy converted during arcing was calculated

$$D = \frac{C}{2} (U^2 - U_0^2). \qquad (3)$$

/30

The capacitance C of the test unit was varied by parallel connections of additional capacitances between 1 and 10 nF. The areas of several burned out sections were determined under the microscope. Figure 17 shows such a burn-out section with arcing channel.

The size of the burned-out section depends only on the magnitude of the energy conversion. All other parameters such as layer thickness, arcing voltage, capacitance, etc. affect only the energy conversion and, in this way, affect the size of the burned-out section /21/. Figure 13 shows the relation between burned-out section area and energy conversion (solid line). This was first found with thicker dielectrics for higher voltages and correspondingly higher energy conversions (crosses in figure 13). These measurements were made with different dielectrics, dielectric thicknesses, and capacitance values. The test described here with the thinnest dielectric layers (circles in figure 13) have now shown that the mathematical relations remain valid down to the smallest discharge energy. The dashed straight line in figure 13 represents the vaporization energy for an average aluminum coating.

One can recognize that of this converted energy a large part, for small energy conversions the overwhelming part, is used for vaporization of the metal. The remaining energy destroys the dielectric in the arcing channel and at the surfaces of the burn-out area /22/. For arcing at the smallest measured energy conversions no more burn-out sections were observed; here only the metal above the arcing channel was removed. Even these locations still had

satisfactory insulation.

The measurements showed further that during arcing the voltage does not drop to below about 17 V but that this lower limit is attained frequently. Figure 14 should make this clear. To produce this /31 a test was conducted with a construction different from the one described. A voltage was applied to a model capacitor via a series resistance of only 1 MΩ. Because of the small time constant the voltage at the capacitor rose, at the connection, very rapidly to the prescribed value which, after every arcing, was again attained just as quickly so that the arcing occurred in close sequence. The lower limit of the voltage decay which was almost obtained in most arcing events can be clearly recognized.

For voltages below the given limit of about 17 V no arcing was observed.

In figure 15 the energy conversions E referenced to the capacity C

$$\frac{E}{C} = \frac{U^2 - U_0^2}{2} \qquad (4)$$

are plotted against the arcing voltage U for the individually observed arcings. The plotted curve corresponds to the case where the final voltage U_0 after arcing is equal to 17 V. Points which lie below the curve correspond to a $U_0 > 17V$. The frequency of the points decreases rapidly with increasing distance. Higher capacitances with correspondingly higher energy content show a tendency to somewhat higher final voltage U_0.

In figure 16 the curve of figure 15 is plotted on a two-cycle logarithmic scale as compared to measurements with capacitors having 6 µm thick polyethylene terephthalate as dielectric. For $U \gg U_0$ we obtain according to equation (4).

(5) $$E/C \approx U^2.$$

In the range $U \approx U_0$ the curve is curved according to equation (4). For the measurement with polyethylene terephthalate we obtained a similar curve, to a large extent independent of the capacitance, which, however aims at a higher limiting voltage for U_0. /32

For the linear relation between burn-out area and energy conversion shown in figure 13 for two-cycle logarithmic plotting one can recognize that, with decreasing energy conversion, an increasing share of the energy is utilized for metal vaporization; the load on the dielectric becomes increasingly lower. Similarly the voltage available for ionization becomes increasingly smaller until, below the critical limit of about 17 V (for the glow polymerized layer investigated) it is obviously no longer sufficient to support an arcing current. Thus for this voltage the self-healing process is terminated. Below it no arcing can occur. This critical limit depends, as can be seen in figure 16, on the thickness of the dielectric and perhaps also on the chemical composition of the dielectric. Below this voltage limit where no self-healing arcing can occur a slow self-healing process becomes effective /23/ which is based on electro-chemical processes.

4. Tests for increasing the deposition speed and improvement of the coating properties

4.1 Introduction

With a view toward economic production of thin layers by means of glow polymerization an effort is made to attain transport speeds as high as possible of the foils through the coating apparatus. This transport speed depends on the one hand on the geometry and the size of the electrodes in the apparatus, and on the other hand, on the deposition speed of the thin layers from the carrier foil.

The geometry of the electrodes was described under 2.1. The connecting in series of several electrode pairs demonstrates the basic possibility to increase the transport speed in this manner and at the same time keeping the thickness of the coating constant.

In preliminary tests (see 2.2) it was already possible to find an optimum with respect to deposition speed and coating properties during the production of polymer layers made of hydrocarbons of the formula $(CH_2)_n$ by varying the various test parameters, such as gas pressure and current density. It occurs at a working pressure of about 300 N/m^2 and at a current density of about 2 mA/cm^2. The optimum is established with respect to gas pressure by the negative influence of foreign atoms, which make their presence known, with increasing working pressure, by increasing embrittlement of the layers resulting from increased cross-linking and shortening of the chain links.

In the following we shall now investigate the effect of the monomer gases on the deposition speed. In these considerations one must take into account that the layers generated are very thin and that the surface capacitances are very great. Thus for producing a certain capacitance from conventional dielectric thicknesses, such as 3 µm, we must produce dielectric surfaces which are 20 times greater than those of a capacitor of equal capacitance with a glow polymerization layer 150 nm thick.

4.2 Choice of the monomer gases

The energy available in glow discharge is sufficient to crack all bondings found in organic substances. It is possible, therefore, to produce layers with given properties by the suitable choice of the monomers and the test conditions. For dielectric applications the following criteria are controlling: good electrical behavior, such as low dielectric losses over a wide frequency range, high temperature constancies of the capacitance, high dielectric

constant, and the ability to employ high field strength; in addition resistance to oxidation, sufficient elasticity, and high temperature constancy.

From these considerations one obtains the requirement for a build-up of the layers as free as possible of dipoles, such as one can find in polyolefins, such as polyethylene and polypropylene, and for perfluorinated polyolefins, such as polytetra fluoroethylene, and polystyrole. These substances are made up of benzene-substituted vinyl groups (styrole, divinylbenzene) resp. from $(-CH_2-)$- or $(-CF_2)$- units. It is necessary, therefore, that the starting monomers are made up of such basic units.

The necessity for regeneration capability poses additional demands on the dielectric. In the capacitor construction (figure 4) very thin metal layers are necessary, for one, and for another, certain prerequisites concerning the chemical construction of the dielectric must be satisfied /22/. Thus, in particular, a certain ratio of carbon to hydrogen- or halogen portions must be satisfied. Figure 17 shows a self-healing arcing in such a regenerating dielectric, for which a highly insulating area is formed around the arcing channel. For the case where the chemical composition of the dielectric contains a greater carbon content, conducting carbon bridges are formed during arcing between the two metallic coatings. According to accurate investigations /22/ benzene derivatives, in particular, are not suited as regenerating dielectrics. This, thus, sets additional limits for the possible substances to be used as starting monomers which during glow discharges form layers with a basic structure made up of $(-CH_2-)$- or $(-CF_2-)$ units.

Thus, for the material groups of the pure hydrocarbons only monomers of composition C_nH_{2n+2} and C_nH_{2n} may be used where the first contained exclusively single bonds in their construction

and thus produced considerably lower polymerization speed than molecules of the composition C_nH_{2n}. Those have either double bonds in the molecule or are made up of a cyclic structure. By means of /35
a single excitation process in glow discharge two free valences are produced by cracking of a double bond or by the split-up of a ring molecule so that in this way excited molecules can be assembled to polymer chains. Molecules without double bonds, on the other hand, must be activated in two places (by cracking or by splitting-off of an H-atom) in order to be able to polymerize. Such a simultaneous double excitation is relatively improbable.

Therefore, the additional investigations concentrated on the series of alkene and cycloalkene. Table 3 lists the most important hydrocarbons with their vapor pressure and their deposition speed for a current density j of 2 mA/cm^2. The deposition speed refers to the static case (carrier belt at rest).

Table 3 Starting monomers for glow polymerization (hydrocarbons)

	relative mass of molecules	boiling point °C	vapor pressure at room temp. N/m^2	deposition speed (nm/s)
ethene	28	-102.4	gaseous	3.5
propene	42	- 47.7	"	5
butene	56	- 6.6	"	7
pentene	70	38.4	$4 \cdot 10^4$	8.5
hexene -1	84	63.5	$2 \cdot 10^4$	10
cyclohexane	84	80.8	$1.2 \cdot 10^4$	10
heptene -1	98	93.1	$8 \cdot 10^3$	11.0
octene	112	≈101	$5 \cdot 10^3$	12.5

Glow polymerized layers could be produced with all these substances.

The polymerization speed of monomers of similar structure depends almost linearly on their relative mass of the molecule (table 1). From that one can conclude that the number of the excitation processes for equal molecule density is almost independent of molecule size. For this reason the investigations were concentrated on monomers of high relative molecular mass. However, one has to take into account that monomer flooding had to be employed. To obtain a sufficient fresh gas supply the monomer pressure had to be about 10 times the working pressure. To obtain a working pressure of several 100 N/m^2 no monomers with molecular mass greater than that of octene could be employed. For heptene- and octene polymerides the chain links are already so large that steric hindrances set in during layer formations, which imparted a certain degree of stickiness to the polymer film because of lacking cross-linking. /36

The most favorable coating properties were obtained with monomers having 5-6 carbon atoms, whereby cyclohexane had the additional advantage, that it can form layers with primarily linear chain structure and relatively few side chains similar to cross-linked polyethylene.

Analogously to the test with hydrocarbons experiments were also conducted with corresponding perfluorinated compounds. Table 4 lists several important data for the polymerization of perfluoro-carbons, also referenced to a current density of 2 mA/cm^2.

Table 4 Starting monomers for glow polymerization (perfluorocarbons)

	relative mass of molecules	boiling point °C	vapor pressure at RT N/m^2	deposition speed (nm/sec)
tetrafluoroethylene	100	-78.4	gaseous	-
hexafluoropropylene	150	-29.4	"	3.5
perfluorobutylene	200	- 8.0	"	5
perfluorocyclobutane	200	- 6.4	"	5
perfluorocyclohexane	300	57	$5 \cdot 10^{3}$	7.5

Even for perfluorinated compounds the law of increasing deposition speed with increasing relative mass of the molecule applies. However, the deposition speed is only about half as great as that for the corresponding hydrocarbons. Except for tetrafluoroethylene coatings were produced from all the above-named substances. Tetrafluoroethylene is difficult to process (danger of explosion) and exhibits the lowest deposition rate. Furthermore, investigations with this substance had already been conducted by others /24,25/. /37

The deposition rate of perfluorinated substances is only about 50% of that of the corresponding hydrocarbons. This results from the lower possible working pressure and from the missing cross-linking reaction. Practically only C-C bonds are broken up. Fluorine atoms are split off only rarely (energy of the C-F bonds 5.4 eV). For that reason the number of the dipoles resulting is also very low. It is the lowest because of the lack of longer side chains for the materials perfluorocyclobutane and perfluoro-dimethylcyclohexane. The electrical properties of these coatings are described in greater detail in section 3. They closely approach the industrial perfluorinated plastics and show that, during glow polymerization of fluorocarbons, very few reactive molecules

(e.g. C = O-groups) are built in. Even the low water take-up (~ 3%o) leads to that conclusion.

In order to obtain the electrical properties described under 3, it is necessary to de-gas the reaction set-up completely, to clean the reaction vessel by glow discharges with an inert gas, and to dry the carrier foil thoroughly. In addition the monomer gases must be dried before admittance into the reaction vessel and must be freed of oxygen by suitable reduction agents.

4.3 Monomer mixtures /38

Polymer coatings made up of hydrocarbons of the formula $(CF_2)n$ exhibit high moisture resistance and low loss factors, those of the formula $(CH_2)n$ exhibit excellent self-healing properties. In order to combine the advantages of both polymers in one coating tests were conducted with mixtures made up of both materials.

For this both material groups were alternately deposited, one above the other, up to 5 polymer layers. The thicknesses of the individual layers could be estimated to be between 5 and 20 nm based on extrapolation of the transportation speed from known thicknesses. The electrical properties of this buildup corresponded to the ratio of the participating individual substances. In contrast to pure perfluorinated layers the regeneration capability is also completely sufficient during inclusion of very thin cyclohexane coatings. In addition, it furnishes the possibility to adjust accurately the temperature coefficient of the capacitance within certain limits by the appropriate selection of layer thickness.

In order to avoid the multiple coating process and to obtain new dielectric layers, the two gas components were mixed by means of mixing devices in the supply tubes and were passed

directly into the discharge zone. The characteristics of the glow discharge changed because of the different polymerization mechanisms of the two gases with the combined compositions.

The many combination possibilities with respect to material selection as well as with respect to mass ratio required extensive testing. It was possible to obtain an optimum of results with respect to production requirements and coating properties. An important result was an increase in the polymerization speed. The most favorable material combination was cyclohexane-perfluorodimethylcyclohexane. For these combinations the partial pressures of the two gases were varied in a test series for a total pressure of 300 N/m^2 each, so that, starting with 100% cyclohexane up to 100% perfluoromethylcyclohexane mixture ratios were obtained in 10% steps. Table 5 shows the deposition speed in nm/s as a function of the gas composition for a current density of 2 mA/cm^2.

Table 5 Deposition speed of gas mixtures

	gas composition (%)										
cyclohexane	100	90	80	70	60	50	40	30	20	10	0
perfluoromethyl-cyclohexane	0	10	20	30	40	50	60	70	80	90	100
	deposition speed (nm/s)										
mixture	10	11	13	14	17	19	18	15	13	10	8

For a corresponding mixture composition the deposition speed increased to about double the value. Similar results, but not so favorable, were also obtained with mixtures from pure hydrocarbons and corresponding fluorinated materials. Here the chemical structure of the two reaction partners need not be necessarily analogous. Thus, for instance, the system propylene-perfluorocyclobutane also has a significantly greater polymerization speed than the individual components. No unequivocal explanation has as

yet been found for the mechanism which brings about the increase in deposition speed. It is possible that a mutual sensitizing and exciting of the molecules takes place since during glow polymerization light of different wave lengths, primarily in the UV range, arises and since the pure and perfluorinated hydrocarbons have different absorption bands.

In addition to the attainment of increased deposition velocity it was possible to vary the electrical and mechanical properties of these films within certain limits. Thus films with 30% perfluorinated gas and 70% cyclohexane have already been found to be elastic up to a thickness of several µm, while layers of such thicknesses made up of cyclohexane alone are very brittle. In addition the moisture sensitivity as compared to pure hydrocarbon has been decreased significantly; on the other hand, the regeneration capability of such layers made up of mixed polymerides is still excellent and the TK_C of such a layer is close to zero. /40

By the use of such gas mixtures whose composition can be adapted to any particular requirement, the possibilities for the application of glow polymerization layers can be expanded considerably.

4.4 Kinetic processes in glow discharge

The effective cross-section of the positive monomer ion with reference to the coating formation process on the electrodes is about 10 times that of the electrons /2, 26/. This can be shown with glow discharge investigations using D.C. where the material polymerized on the cathode is several times that polymerized on the anode. At the same time it is found from these tests that the polymerization to macromolecules for a given pressure and suitable current densities takes place overwhelmingly directly on the surfaces of the electrodes. Since the molecule density in the gas volume is low, the probability of stacking together a series of molecules to a polymer chain is not realistic.

The short chains that are produced are carried off by the gas stream and sucked off.

In the following we shall describe in greater detail the processes in the plasma with the aid of kinetic gas theory.

For the average square of the velocity of the molecules in the reaction chamber we obtain

$$\bar{u}^2 = \frac{3kT}{m} \qquad 1$$

(k Boltzmann's constant, T temperature in K, m mass of the molecule)

The average velocity $\bar{u}$ is:

$$\bar{u} = 0{,}921 \cdot \sqrt{\bar{u}^2} \qquad (2)$$

The average free path lengths of the molecule λ_m between two collisions is

$$\lambda_m = \frac{1}{4\pi \cdot \sqrt{2}\, N r_m^2} \qquad (3a)$$

(r_m radius of molecule, N number of particles/volume)

Compared to the radius of the molecule of several 10^{-10}m the radius of the electron of $2.8 \cdot 10^{-15}$m can be neglected. For the free path length λ_{el} of the electrons (3a) simplified according to the kinetic gas theory to

$$\lambda_{el} = \frac{1}{\pi N r_m^2} \qquad (3b)$$

The temperature T in the reactor can be assumed to be about 300 K.

From the above relations, the monomer-specific working pressure and the density of the liquid monomers, we obtained important data (table 6) for the reactions occurring in the plasma. These data were calculated for the hydrocarbon cyclohexane and for the perfluorinated cyclobutane for whose coating a large number of tests

is available.

Table 6 Gas kinetic data of cyclohexane and perfluorocyclobutane

		Cyclohexane	Perfluoro-cyclobutane
Radius of molecule r	nm	0.35	0.37
Average velocity $\bar{u}$	m/s	274	178
Average free path lengths λ_m	µm	5.3	7.7
Free path lengths of the electron λ_{el}	µm	30	44

Since the electrons, based on their low mass, lose practically no energy in elastic collisions with gas molecules, they take on a quasi-thermal velocity corresponding to several eV. Starting with this velocity level they are accelerated by an applied electric field $\vec{E}$. They obtain the maximum possible energy addition from two collisions, if the original flight path and direction of the electrical field coincide:

$$\Delta\varepsilon = e \cdot \vec{E} \cdot \lambda_{el} \qquad \begin{matrix}(e \text{ elementary charge,} \\ E \text{ electrical field strength})\end{matrix} \qquad (4)$$

For a maximum field strength of about $3 \cdot 10^4$ V/m this means an energy increase of about 1 eV between two collisions. Thus, the energy of the electron increases with each individual elastic collision until it can be transferred to a molecule by an inelastic collision, e.g., for the excitation or dissociation of a light electron or for cracking of a molecule bond. As can be seen from section 5.4 an energy of about 3.7 eV is required for breaking up a C-C single bond; for splitting off the H-atoms 4.3 eV are required. During splitting off of two bonds of a cyclic molecule low molecular cracking products are produced. By the

dissociation of H-ions branching to larger molecules takes place.

For perfluorinated substances 5.4 eV are necessary for splitting off a fluorine atom; i.e., the colliding electron, in the absence of inelastic collision, must be accelerated more often in order to attain this energy. The probability for this is considerably lower; in addition free fluorine atoms are very reactive and attached to other molecules. These different bonding energies explain not only the results of the mass spectrometric investigation in section 5.4, but also the varying coating properties of the resulting polymers as will be discussed in a different place.

The excitation processes by ionized molecules, principally /43
cations, play a relatively small role in the discharge volume, since, based on their shorter free path lengths according to (4), they would have to pass through a greater number of excitation steps without neutralization by electrons in order to be able to transfer sufficient activation energies. However, according to the experimental results, they are responsible for the major portion of the polymerization processes on the electrodes.

Apparently the main polymerization process first starts on the electrode surface. The molecules colliding with the electrodes are adsorbed in part. For hydrocarbons the heat of adsorption is greater than the heat of condensation /25/. In addition the vapor pressure of the monomers used is greater than the working pressure prevailing in the reactor by a factor of 10. Therefore, at equilibrium a monomolecular layer of the surfaces to be coated will take place. In glow discharge monomer cations impact on the electrodes and initiate a polymerization process. By this process the surfaces are changed, the diffusion equilibrium is disturbed, and a new molecular layer can be deposited.

The time- and area-dependent number z of the colliding

molecules is given by the pressure p. We have

$$p = z \cdot 2m \sqrt{\bar{u}^2}, \quad \text{and}$$

$$p = \frac{1}{3} Nm \bar{u}^2;$$

from this it follows:

$$z = \frac{1}{6} N \sqrt{\bar{u}^2} \qquad (5)$$

For cyclohexane we obtain $z = 4.35 \cdot 10^{20}$ molecules/cm^2·s, for perfluorocyclobutane we obtain correspondingly $z = 1.7 \cdot 10^{20}$ molecules/cm^2· s.

A current density of 2 mA/cm^2, corresponding to the deposition speed listed in the table , is identical with a flux of $12.4 \cdot 10^{15}$ elementary charges per cm^2 and seconds. Half of them are cations, half of which again collide on 1 cm^2 electrode surface (since the two surfaces face each other). Thus, the cation flux is

$$I^+ = 3.1 \cdot 10^{15} K^+/cm^2 \cdot s$$

Of about 10^5 molecules which impact on the electrodes, only one is thus a cation so that the thermal diffusion process at the electrode can proceed practically without disturbance.

For cyclohexane, with the assumption of an adsorbed monomolecular layer on the electrode in equilibrium, we obtain a coverage density of $2.3 \cdot 10^{14}$ molecules/cm^2 (the diameter of a cyclohexane molecule is about $7 \cdot 10^{-10}$m /27/). The average dwell time τ of an adsorbed molecule on the electrode then becomes: τ = adsorbed molecule per cm^2/colliding molecules per cm^2 and seconds; i.e.

$$\tau = 5{,}4 \cdot 10^{-7} s \approx 5 \cdot 10^{-7} s$$

From the density of about 1 g/cm^2 of the deposited materials and a measured growth velocity proportional to the current strength of 5 $\frac{nm \cdot cm^2}{mA \cdot s}$ we obtain for cyclohexane for the above current strength

a deposition rate M of $7 \cdot 10^{15}$ molecules cm^2 s. This means about 30 molecule layers with a thickness of $3.2 \cdot 10^{-10}$m per molecule.

The specific polymerization rate, referenced to the number of the polymerized molecules per colliding positive monomer ions is

$$\frac{M}{I^+} = 7 \cdot 10^{15}/3.1 \cdot 10^{15} = 2.25 \text{ molecules/cation.}$$

During the estimated dwell time of $5 \cdot 10^{-7}$ s of the adsorbed molecules they can react with one another on the surface, and in such a way that they can collide directly with an ion since the factor $M/I^+ > 1$. /45

The polymerization speed of perfluorocarbons is, under the same conditions (pressure, current strength), only about half as great as that for the equally great hydrocarbons build up in the corresponding mass. The splitting-off of fluorines is very low, and based on the high reactivity of fluorines the recombination rate of fluorines is very high so that no additional polymerization possibilities arise to reactions with side chains.

5. IR spectroscopic and mass spectrometric investigations

5.1 Introduction

In glow polymerization processes primarily ions and different radicals with free valences are produced in a gas discharge volume. The relative frequency of these radicals in a gas phase control decisively the chemical structure and the physical properties of the thin polymer layer since free valences in the chain molecules can cause the formation of branch points or an inclusion of polar atom groups by conversion with O_2 or H_2O. Since the prevailing physical polymerization differs here basically from the known chemical polymerization processes, one can predict which type of materials are produced not only with respect to chemical composition

but also with respect to structure. Therefore, an investigation of these new materials was necessary. As methods of analysis the IR absorption spectroscopy suggests itself with which molecular structures in organic compounds can be proven specifically with the aid of characteristic absorption and in this way, for new synthetic polymer compounds, detailed information concerning the chemical composition can be obtained.

In addition to the glow polymerization layers the gases pumped from the gas reaction volume are also analyzed in order to obtain information concerning the composition of the plasma. /46

5.2 Experimental with respect to the IR investigations

As substrate for the thin dielectric layers we utilized each time metallized plastic foils (Hostaphan 50 µm). For the analyses an IR absorption spectrophotometer model 21 of Perkin-Elmer was available with which IR spectra in the wave length range 2-15 µm could be obtained. In most cases an analysis of the layers by the conventional penetration radiation method was impossible because, based on the very low thicknesses of the samples, no actively measurable absorption signals were possible on the one hand, and, on the other hand, the layers could not be separated as a rule from their metallized substrate. Thus an important aid to these investigations turned out to be the method of the attenuated multiple IR spectroscopic total reflection (FMIR-Technology) in which on both sides the multiple total reflection occurring in the boundary surface between a planar parallel crystal made of thallium iodide with high index of refraction and the thin sample layer was utilized. The method depends on the fact that the radiation, for each total reflection, penetrates the optically thinner medium of the probe layer at a lower depth ($\sim$ 0.1 µm) and that it is attenuated here by absorption as well as by penetrating radiation of a corresponding layer before it returns into the optically thicker medium of the crystal /28/. The absorption effect

in the sample layer is amplified with each additional total reflection so that the light portions emitted at the end of the FMIR unit represent, as a function of wave length, the exact image of absorption spectrum of the sample layer obtained with greater coating thickness.

5.3 Results of the IR investigations

The investigations extended to dielectric layers for whose production various linear as well as cyclically constructed hydrocarbons- and fluorocarbon monomers were used (see tables 3 and 4). /47

The IR spectra of the dielectric layers produced from C_3H_6 and C_6H_{12} exhibited the same main absorption bands whose characteristics are listed in table 7.

Table 7 Main absorption bands of the IR spectra of glow polymerides from hydrocarbons

Bands	wave length ranges (µm)	rel. absorption intensity (rough markings)	associated oscillations according to /30/
1	3.35 - 3.50	strong	CH_3-, CH_2-. CH-valence
2	5.8 - 5.9	average	C = O-valence
3	6.85 - 6.9	average	CH-deformation in $-CH_2-$ and asym. $C-CH_3$
4	7.25	average	CH-deformation in sym. $C-CH_3$

Except for band 2, both spectra correspond to the spectrum of a long chain aliphatic hydrocarbon polymer without crystalline contributions /29/. Thus from C_3H_6 and C_6H_{12} dielectric layers

are produced by glow polymerization with extensively equal chemical structure. From the intensity of band 4 one can conclude that in both cases CH_2-chain contained a considerable number of branch points with CH_3 - groups /30/. Peak 2 proves the existence of C=O-groups which are apparently produced during the glow discharge by a conversion of the gas phase with H_2O molecules adsorbed on the substrate and which, because of their polarity, produce an increase of the dielectric losses and the water take-up of the layers. A quantitative comparison of the two spectra showed that these oxidated portions were present in smaller amounts in the coating produced from the cyclic monomer C_6H_{12}.

The IR spectra of the polymer layers formed from C_3F_6, C_4F_8, and C_8F_{16} also agreed completely with one another; the data are listed in table 8. /4

Table 8 Absorption bands of the IR spectrum of glow polymerides from fluorocarbons

Bands	range of wave length (µm)	rel. absorption intensity (rough markings)	associated oscillations according to /30/
1	5.7 - 5.9	weak	C=O-valence
2	8.1 - 8.6	strong	CF_2 - valence
3	10.2	weak	CH-wagging in vinyl groups
4	13.4 - 13.8	average	$CF-CF_3$-valence

Just as the spectrum of polytetrafluoroethylene /29/ the spectra of these thin layers exhibit a main absorption band at 8.1 - 8.6 µm (Peak 2). This clearly points to the fact that during the glow polymerization of the named fluorocarbons we obtain overwhelmingly CF_2-chains. A difference compared to polytetrafluoroethylene lies in the fact that the glow polymeride - as can be seen

from the magnitude of peak 4 - contain more $CF-CF_3$ members. As in the polymerization of hydrocarbons, C=O-groups are also built in during the polymerization of fluorocarbons; this can be seen from the appearance of peak 1 (table 8). The controlling conversion of adsorbed H_2O molecules produces as an intermediate product hydrogen which - as shown by peak 3 - is bound chemically in the polymer layer.

The IR spectroscopic investigations showed that neither for hydrocarbons - nor for fluorocarbon polymerization the replacement of linearly built-up starting materials by monomers with cyclic structure produced a change of the chemical composition of the thin layers.

To increase the deposition speed as well as to obtain layers with selected dielectric properties it is of advantage, (see also 4.4), to generate in the glow discharge process co-polymerides through the use of mixtures from hydrocarbon- and fluorocarbon monomers. /49

In the IR spectroscopic investigations of such a co-polymeride made up of C_6H_{12} and C_8F_{16} it was found that both monomers were connected to each other in an essentially homogeneous distribution to form chains.

5.4 Mass spectrometric investigations

During the polymer layer formation on the electrode there arise in the gas discharge volume a series of cracked products whose mass is lower to a large extent than that of the starting substance. Since they supply important information with respect to the composition of the plasma, they were analyzed mass spectrometrically. As an example let us use propene (figure 18). In addition to a strong hydrogen band one can also find all possible radical combinations up to 6 carbon atoms. The other radicals C_2H_2, C_2H_3, C_2H_4 and the propane radical C_3H_3 were especially abundant. The remaining radicals cannot be identified individually

because of the decreasing resolution power of the spectrometer with increasing mass. The H_2O band showed that, even for careful drying of the built-in parts and of the carrier foil, residual water molecules cannot be excluded.

In mass spectrometric analyses of the other hydrocarbons it was found that the spectra can be differentiated only quantitatively, but not qualitatively. However, the mass spectrograms of the perfluorinated combinations used hardly show any evidence of crack products. For perfluorocyclobutane (C_4F_8), only a very weak peak for F_2 and the radical CF_2 and C_2F_3 can be identified.

The difference in compositions of the plasmas of the two material groups (pure hydrocarbons as opposed to perfluorocarbons) can be explained by the different bonding energy in the molecular structure. Thus one needs for

opening of a C=C-bond	about 2.6 eV
break-up of a C-C-bond (aliphatic)	about 3.7 eV
break-up of a C-H-bond	about 4.3 eV
break-up of a C-F-bond	about 5.4 eV

/50

6. Adhesive strength investigations

6.1 Introduction

The thin glow polymerization layers which are produced on a carrier band can only be processed further to capacitors on this carrier. This results in capacitor construction as shown in figure 19 and 21.

The capacitor thus consists of a carrier foil and 2 or 3 layers applied in succession (metallizing, glow polymerization layer, and possibly also a second metallizing). This type of construction poses high demands on the adhesion of the individual layer.

Thus the metal layer vaporized on the carrier foil experiences a high temperature and mechanical stress during the application of the glow polymerization layer which must not produce a separation or change of the metal cover on the carrier. Even during the second metallizing process the layers lying below it are stressed highly. Carrier foils, glow polymerization and metal layers have greatly different expansion coefficients which, during temperature changes, lead to mechanical stresses. As is well known, the foils from carbohydrates and fluorocarbons, related to the glow polymerization layers, have very poor adhesive properties. However, since between metal cover and carrier foil as well as between metal cover and glow polymerization layer a very good adhesion must be guaranteed during the production and in continued use, corresponding investigations were conducted.

6.2 Adhesion problems between carrier foil and metal cover /51

6.2.1 Relation between surface tension and adhesion

To gain an idea as to which plastic foil, based on their properties (temperature resistance, water take-up, surface tension) are suitable as carriers for the glow polymerization layers, systematic investigations were conducted with the foils (polyethyleneterephthalate-, polycarbonate-, polypropylene-, fluoroethylenepropylene-, polyimidefoil) in question.

With respect to adhesion of the metallized layer on the carrier foil its surface tension is controlling. We therefore searched for a method with which this could be determined quickly and with sufficient accuracy. The choice was a so-called Union-Carbide-Test. For this, mixtures were prepared from formamide and ethyleneglycol-monoethylether, each with widely varying mixture ratios, but definite surface tension. This test liquid is brushed onto the surface of the test unit . The test unit then possesses the surface tension of that test fluid which remains on the surface

for 2 seconds with sharply defined edges, without contracting or without spreading.

According to this measuring method, of the listed dielectric, FEP (fluoroethylenepropylene) has the lowest surface tension of about 20 mN/m. Then follows polypropylene with a surface tension of 30...31 mN/m. Polyethylene terephthalate, polycarbonate and polyimide belong to those materials which, already without any pretreatment of the surface, have a surface tension of 42... 45 mN/m.

Investigation of the metallizing capability of the foils showed that the adhesive strength of the metal on the surface as well as its condensation rate depend on the surface tension of the foil. Thus, for identical vaporization parameters less than half of the metal condenses per unit time on FEP then on polyethylene terephthalate. More accurate conductivity measurements of the /52
vaporized metals showed that, for good condensation requirements the surface tension must be at least 35 mN/m. For the adhesive strength of the Al-coat we obtain a steep increase between 35 and 40 mN/m.

The adhesive strength was measured by first pouring epoxy resin blocks onto the foil and subsequently peeling off the foil from the blocks with measurement of the required force. For this foil strips of about 1 cm width were cemented on the metallized side (e.g. aluminum) with epoxy resin blocks. The adhesion between epoxy resin block and metal was always greater than the adhesion of the metal on the foil surfaces. It was determined empirically that for the production of capacitors an adhesive strength of the metal layers on the plastic foil with a tear-off force of 2 N/cm is sufficient. As described in the following, this tear-off force can be achieved for polar foils without pretreatment, for unpolar foils by glowing or by sputtering.

6.2.2 Methods for improving the adhesive strength of thin metal layers on plastic foils

Polar carrier foils possess a sufficient surface tension so that metal vapor deposition is possible without special surface treatment. However, they are often prone to greater moisture pickup which can affect the adhesive strength of the metal layer. Thus, for instance, polyimide, has a high surface tension and an excellent temperature constancy, so that during the vaporization process no thermal decomposition products are produced. Its moisture pickup, however, is considerable (about 3%). Thus, before metallization polyimide must be dried for about 1 week at 100° under vacuum. If one omits this step then, during vaporization with metal under high temperature stresses, the water vapor present in the foil evaporates and forms an intermediate layer of metal-hydroxide between foil and metal. This intermediate layer prevents a satisfactory adhesion of the metal. In addition a glowing /53
bluish discoloration of the metal coat becomes visible which can be attributed to partial oxidation. An improvement of adhesion of metal layers on unpolared foils could be achieved by measures in which polar groups or condensation nuclei were generated on the foil surface to which the metal atoms could adhere. This can be done, e.g., by exposure to glowing in an oxygen-containing atmosphere, in the same apparatus in which the just described polymerization processes take place; or one can expose the carrier foil to a so-called "silent discharge" at atmospheric pressure. The best results were achieved when the foil was previously subjected to a sputtering process. For a sputtering material we used either the same metal as was used for vapor deposition (primarily aluminum) or a metal with higher atomic weight, such as nickel. The metal atom penetrates during sputtering into the soft plastic surface; the penetration increases with increasing atomic weight. The sputtered metal quantity can be extremely small (no cohesive, conductive layer need be formed). During the subsequent metallizing the sputtered atoms act as condensation

nuclei and effect a firm clamping of the metal coat with the carrier foil. In general, surfaces which can be easily metallized have good adhesion, such as epoxy resin. Non-pretreated polypropylene surfaces do not, for instance, adhere to epoxy resin. However, if one pours onto the sputtered polypropylene epoxy resin, hardens it and attempts subsequently to pull the foil off the epoxy resin, the foil tears and the polypropylene layer remains on the epoxy resin block.

The most detailed investigations for improving adhesive capability by means of sputtering were conducted with fluoroethylenepropylene (FEP). Nickel was used as the sputtering material. The following correlations between sputtered nickel layer and the forced pull-out of the aluminum layer was found. /54

Table 9 Adhesion of Al-vapor deposited layer on FEP as a function of a sputtered intermediate layer

Thickness of the nickel Layer	Force required to pull off the Al-layer (vapor deposited)
0.13 nm	1.8 N/cm
0.25 nm	2 N/cm
0.5 nm	3 N/cm
0.75 nm	3.1 N/cm
3 nm	4 N/cm
30 nm	4 N/cm

It was sufficient to sputter on a few atomic layers of a metal. This did not measurably increase the surface conductivity of the plastic foil; however, the adhesive strength of the metal electrode vaporized onto it was sufficient.

6.3 Adhesion problems of the polymer layer on the metallized carrier

6.3.1 Increase of the adhesion strength of layers by means of dipole containing structures in the monomer gas

For dielectric layers with a thickness below 0.3 µm adhesion on the metallized carrier by means of the measures described in the fourth section, such as de-gasing of the reaction vessel, drying of the carrier foil, and the removal of water and oxygen from the monomer, was already sufficient to be able to employ them as capacitor dielectrics.

To improve the adhesion strength of thick layers adhesion promoters had to be used. Silanes are an example of promoters between organic and inorganic layers. A direct application of such compounds onto the metal surface, however, brought no improvement of adhesion. Therefore, an attempt was made to start directly from the glow discharge and to achieve the desired /55
effect by the addition of monomer gas. These additives must possess a high dipole moment in order to bond with the substrate and, by themselves, make worse the electrical properties of the glow polymeride. Therefore, only extremely thin boundary layers (≤5 nm) were provided with dielectrically unfavorable additives. The procedure was such that in a supply container material, such as silane, organic substances (e.g. aldehyde, alcohol) or mixtures thereof were mixed in a ratio of 1 : 10^3 with the monomers for the glow discharge. This mixture was then added to the main gas stream which led into the discharge apparatus. For a working pressure of about 1 mbar the partial pressure of the additives could be controlled down to 10^{-5} mbar.

The improvement in adhesion that was achieved by the formation of such a mixture in the boundary surfaces, was sufficient in conjunction with the cited measure for improving

the layer quality for dielectric thicknesses ≤0.5 μm. At the present state of development thicker layers are of no great importance.

6.3.2 Occurance and prevention of separating layers between metal coatings and glow polymerides

Thicker carrier foils with sufficient temperature resistance (> 150°C), such as polyethylene terephthalate, could be vapor deposited with aluminum to form adhesive coatings with any required conductivity, for capacitors, up to 20 S/□ (0.7 μm). Thermally sensitive foils, such as polypropylene of 6 μm thickness or even thinner carrier foils (~ 3 μm) from polyethylene terephthalate, which were to be used in capacitors for reason of high energy density, could not be wound as problem-free during the metallization process as thick foils. Thus, for instance, wrinkles developed which did not have a heat conducting contact with the cooling roller during the metallization process. In these places overheat damages can arise during the production of thicker vapor deposit layers. These can not be seen directly. They lead to a poor adhesion of the glow polymer layer on the metal coating. As shown by investigations the poor adhesions can be attributed to intermediate layers which form from the decomposition product from the carrier foil during the metallization process. /56

By means of tests the limits of the coating thicknesses were established below which the thermal stresses were so low that no decomposition product from the carrier foil developed and that, thus, no separating layer arose. For the most often used vaporizing metal aluminum the limit for thin polyethylene terephthalate was 1.5 S/□ , for polypropylene 1 S/□ .

As shown by infrared spectroscopic analyses the polymerization-deposited layers differed from each other as a function of the metallizing thicknesses lying below. As an example let us compare

the hexafluoropropylene layers which were deposited on 2 different polyethylene terephthalate carriers. One carrier was metallized with 1 S/□ , a second one with 10 S/□ . The extinction curves of the two samples were considerably different.

Practically only the bands of the C F-oscillation at a wave length of 8.2 μm and the CF-CF_3 oscillation at 13.8 μm were identical. In all cases a band appeared at 5.8 μm for the C=O-valence oscillation which, however, was considerably weaker for the first sample (thin metallizing) than for the second one. The C=O bands could be attributed, in part, surely to oxygen containing impurities in the starting monomers and to the O_2 partial pressure in the glow discharge. For the second sample, however, the predominating part came from the carrier foil. Furthermore we found in this sample, bands at 9.1 μm, 10.3 μm, 11.5 μm, 11.8 μm, which are typical for the decomposition product of polyethylene terephthalate.

7. Production of capacitor prototypes /57

7.1 Introdution

In parallel with the development of the technology of their production the thin glow polymerization layers were also tested for their application potential as capacitor dielectrics. In order to keep the expenditures for coating development as low as possible, many important tests, as described before, were made with model capacitors (3rd section). However, in order to be able to test the behavior of industrial capacitors, the production of such capacitors and their testing was necessary. Thus, for instance, the problem of contacting of the thin metal layers as well as the endurance behavior had to be tested with industrial capacitors. For that purpose 2 types of wound capacitors were produced which are described in the following.

7.2 Production of wound capacitors

The steps for achieving such wound capacitors were as follows: first plastic carrier foils were vapor treated in several capacitor path width with aluminum in the form of strips. The conductance of the metal layer on the active capacitor surface was between 0.2 and 0.5 S/□. The edge of the metal layer to be contacted always had a conductivity > 0.5 S/□. This was followed by the application of a glow polymerization layer across the entire width of the foil. Subsequently, the wide foils were cut into small strips and wound together as shown in figure 19. The front faces of these windings were contacted with conventional Schoop methods; one connecting wire each was then soldered to these front-side metal spray layers. Subsequently, the capacitors were dried and built into aluminum tubes with epoxy resin seals at the front side. As dielectric layer we used predominantly glow polymeride made from cyclohexane because of its high deposition speed, as described in section 4, and its good regeneration capabilities. Its dielectric /58 constant was about 2.5. As carrier foil we used 6 µm polypropylene in the first test. For a dielectric layer thickness of 50 nm on each carrier we obtained a physical volume capacitance (capacitance per effective volume range) of 17 $\mu F/cm^3$. In this construction the capacitance of the carrier foil is parallel to the capacitance of the thin layer and contributes about 2% to the total value.

By switching to the mechanically and thermally more stable polyethylene terephthalate it became possible to coat even 3 µm thick carrier foils without problems. For equal dielectric thickness (2 x 50 µm) physical volume capacitance could be increased to 34 $\mu F/cm^3$.

An additional increase of the volume capacitance was obtained when the construction of the capacitor was changed in accordance with figure 21. For this the entire capacitor system,

consisting of 2 metal coatings with an intermediate polymer layer, was applied in a multiple path width onto a single carrier foil (figure 20) and subsequently separated into individual paths. In this way, the air space, which in a construction as shown in figure 19 reduces the capacitance for extremely thin dielectric layers appreciably, was eliminated by a metallizing process onto the dielectric. The use of only a single foil produced technical advantages during the winding process.

The capacitors of this construction had, for instance, with a carrier foil thickness of 3 µm and a dielectric thickness of 110 nm a physical volume capacitance of 68 $\mu F/cm^3$. This volume capacitance is greater than those obtained in capacitor technology with organic dielectrics by a factor of about 3.

Because of their favorable volume capacitance and the technical advantages during winding the subsequent investigations were conducted only with capacitors which were produced from a single carrier foil. Here the technical construction of the capacitors was as follows: /59

From the foiled path, as shown in figure 20, 10 mm wide strips were cut and were processed into round coils. For insulation- and contact protection several empty starting and end reel sections made of insulation foil were wound on. By spraying on of an aluminum layer onto the front faces of the coils (methods according to Schoop) the thin vapor deposited electrodes were contacted. A white metal layer was sprayed onto this aluminum layer in order to produce a layer for the connecting wires which could be soldered or welded. After the wires had been soldered to the sprayed-on metal layer the coils, as described, were installed into aluminum tubes with epoxy resin seals on the front side.

For the tests conducted a magnitude of the capacitance was 5 to 10 µF. As dielectric we used exclusively polymerized cyclohexane with a thickness of 110 nm. Typical exterior dimensions

of a capacitor built into aluminum tubes with a capacity of 8 μF were diameter of 7 mm and length of 20 mm.

7.3 Capacitor properties

The properties of the capacitors are determined not only by the thin polymer dielectric but they are also affected considerably by the relatively thick carrier foil. Loss factor, behavior during over-voltage, and dielectric constants are predominantly properties of the glow polymerides. The temperature coefficient of the capacitance, the behavior during temperature shocks and during constant exposure to increased temperatures are primarily determined by the carrier material.

The expansion coefficient of the carrier foil ($+140 \cdot 10^{-6}/K$) is larger than that of the cross-linked glow polymeride. One can recognize the lower coefficient of expansion of the glow polymeride by the behavior of the coated carrier foil during temperature changes. During cooling the carrier foil contracts more than the /60
dielectric layer and shows a tendency to roll up in such a way that the polymerization-deposited layer is found on the outside. As a mark of quality one can consider the behavior during temperature shock. The capacitors were exposed in temperature change tests each time 30 minutes to a 100° C environment and 30 minutes to a -40° C environment without intermediate storage at room temperature. Here, after only a few changes, about 20% of the construction elements exhibited insulation decreases to below 10 MΩ , which can be attributed to the mechanical deformation of the coils by the effect of temperature.

These insulation drops, however, can be avoided if the capacitors are subjected to a tempering process at 130° C to 140°C for one hour with a simultaneous application of 20 V_{eff} alternating voltage. Presumably, weak places in the dielectric become evident here and are healed by the applied voltage. After this treatment the insulation values were, even after 50 shock-like temperature

changes between -40°C and +100° C, above 10 000 MΩ x μF.

The temperature coefficient of the capacitance (TK_c) of capacitors with a glow polymeride made of pure hydrocarbon is positive (figure 22) and lies in the temperature range -20° C...+25°C between +500 and +600 · 10^{-6}/K (1 kHz). The positive TK_c results from dipoles in the dielectric; it is still increased because of the higher coefficient of expansion of the layer carrier as compared to the cross-linked glow polymeride (see above).

The frequency dependence of the capacitance is the highest at low temperatures and decreases uniformly to higher temperatures. At -40° C the decrease in capacitance for an increase of frequency by a factor of 10 is about 1%, at +100° C it is only 0.3 to 0.4%

Loss factor measurements with capacitors of such great /61
capacitance could be conducted up to 10 kHz. The inner resistances of the measuring instruments are too high for investigations with higher frequencies. However, already at 10 kHz the loss factor is increased because of the resistance of the coatings and the connecting lines. Figure 23 presents the loss factor curve for the temperature range from -40° C...+100°C.

It can be seen that the tanδ in the temperature range investigated shows no sharp maxima. Even measurements up to 150° exhibit similar loss factor values. This behavior can be attributed to the amorphous structure of the layers and the irregular length of the side chains which thus become mobile at different temperatures.

The dielectric loss factor is a sensitive proof for the degree of purity of the glow polymeride. If during the coating process the supply of fresh gas is too low, which can not necessarily be determined by the growth rate and the thickness uniformity,

then the loss factor increases over the entire range investigated. Basically various properties, such as moisture behavior and capacitance changes during storage at elevated temperature, can be improved by vacuum tempering at 150°C (1 to 2 hours) directly after the production. This improvement is probably based on the fact that, at first, there are present in the layer radicals with unsaturated valences, which become saturated during tempering and which stabilize the layer.

All the results described here were obtained with layers from hydrocarbons of the formula $(CH_2)_n$. The dielectric properties can be improved considerably if one resorts to perfluorinated monomers during the production of the coating (section 3).

Regeneration difficulties developed, however, which prevented /62
a sufficiently high insulation in a compactly wound capacitor of large capacitance (in contrast to the model capacitors described in section 3). The cause for these difficulties is presumed to be the high temperature stability of the dielectric coating which is considerably greater than that of the carrier foil. It seems that, if a weak place with poor insulation and high current glow forms, the carrier foil will heat up to such an extent, before the self-heating process with vaporization of the dielectric and the electrode sets is, that local melting zones are formed which release irreversible short circuits even in the thin dielectric layer lying above it. In order to avoid these difficulties capacitors with layers made of monomer mixtures (pure hydrocarbons and perfluorocarbons) were produced as described in section 4.

By means of these layers coils of great capacitance with satisfactory insulation ($\geq$ 1000 MΩxμF) and low loss factors ($\tan\delta_{1\ kHz} = 2 \cdot 10^{-3}$) were achieved. In addition a TK_C of close to 0 could be established.

7.4 Duration tests with capacitors

To investigate the capacitor properties it is also necessary to conduct endurance tests. The difficulty in the case of the present development lies in the multiplicity of the possible parameters and the frequent changes which had to be made not only in the production of the dielectric layers but also for that of the capacitors. The effect of each one of these changes can only be evaluated after endurance testing, regardless of potentially excellent final values.

In order to reduce the large number of possibilities to an economically and technically justifiable measure, the endurance tests were limited, based on preliminary tests, to capacitor construction with a single foil and with a dielectric made of polymerized cyclohexane. In all cases the thickness of the dielectric was 110 nm. As protection against coating corrosion the test coils were installed into aluminum tubes with front-side epoxy resin seals and then, as described, were tempered under voltage. /63

The following tests were conducted with capacitance values between 5 μF and 10 μF:

Room temperature	12 V= and 10 V~
70°C	12 V= and 0 V
85°C	12 V= and 0 V
100°C	12 V= and 0 V

A stress loading with 12 V signifies for these thin coatings of only 110 nm thickness a field strength of 110 V/μm. For continued operation such field strengths were only obtained in a few cases with capacitors with thicker dielectric.

The voltage-free storage at elevated temperatures should show whether, for instance, fault locations are formed by changes

in the dielectric or by mechanical stresses. Such fault locations can lead to lower insulation if a subsequent voltage stress is so low that it does not lead to self-healing arcing. For low endurance voltage stresses for which no self-healing arcing takes place, a sufficient insulation is assured by means of the electrochemical self-healing /23/.

Tests at room temperature showed, for voltage free storage, capacitance decreases of several % in 5000 hours where the reduction process is essentially completed after 1000 hours. Changes in insulation- and loss factor were not observed here. Stresses at 10 V ~ (50 Hz) and 12 V= produced the same capacitance curve; the time constant of the insulation had values above 10,000 s.

Endurance tests at elevated temperatures also produced no appreciable changes. Table 10 shows the insulation value and the changes in capacitance after 5000 hours under the stated conditions.

Table 10 Change in capacitance and insulation resistance after 5000 hours

	70°C		85°C		100°C	
	0V	12 V	0 V	12 V	0V	12 V
Change in capacitance (%)	-0.8	-0.8	-1.3	-1.4	-2.4	-2.5
Time constant of the insulation resistance (s)	25,000	25,000	18,000	20,000	16,000	20,000

For insulation we are dealing with average values measured at room temperature and for a field strength of 100 V/µm. The insulation values decreased slightly with increasing endurance test temperature and are somewhat lower in voltage free storage than during operation under voltage. These differences are already

pronounced after several 100 hours. Beyond that no important changes can be observed and the insulation remains at a high value.

Similarly, the changes in capacitance have ended to a large extent after 1000 hours. They result from two effects. First, the shrinking of the carrier foil contributes to the decrease in capacitance. This is evidenced by the fact that more tightly wound capacitors also exhibit lower decreases in capacitance. In the second place the DZ of the polymerized dielectrics seem to decrease somewhat. Presumably chemical groups present in the /65
polymeride with higher dipole moment (e.g. double bond) still decrease their dipole moments afterwards by saturation processes.

The chemical conversion processes, however, are not sufficiently significant that they result in a lowering of the dielectric loss factor. This remains constant during the test duration named within the framework of measuring accuracy.

The further continuation of these endurance tests produced after till now 10,000 hours,no more essential changes with respect to the above named tabulated values for capacitance and insulation; and also no worsening of the loss factor.

Appendix 1

References:

/1/ E.G. Linder, A.D. Davis, J. Phys. Chem. 35(1931) 3649.

/2/ R. Haefer, A.A. Mohamed, Acta Phys. Austr., 11(1957) 193.

/3/ H. Carchano, Journ. of Chemical Physics, 61 (1974) 3634.

/4/ A. Bradley, J.P. Hammes, J. Electrochem. Soc., 110 (1963) 15.

/5/ M. Stuart, Proc. IEE, 112 (1965) 1614.

/6/ R.A. Connell, L.V. Gregor, J. Electrochem. Soc., 112 (1965) 1198.

/7/ P.B. Weisz, J. Phys. Chem., 59 (1955) 464

/8/ G.L. Gallet, R. Nannoni, P. de Valance, L'Onde Electrique, 50 (1970) 113

/9/ T. Hirai, O. Nakada, Japanese Journal of Applied Physics, 7, 2 (1968) 112

/10/ S. Nahyama, T. Shiba, V. Mizoguchi, Nec Res. and Dev., 21 (1971) 24.

/11/ H. Kobayashi, A.T. Bell, M. Shen, J. Appl. Polym. Sci., 17 (1973) 885.

/12/ P. White, Proc. Chem. Soc., (1961) 337.

/13/ T. Williams, M.W. Hayes, Nature, 209 (1966) 769.

/14/ Stetter, G.: Dissertation TU München 1964.

/15/ F. Seitz, The Modern Theory of Solids, McGraw Hill, New York (1940).

/16/ I. Frenkel, Phys. Rev., 54 (1938) 647.

/17/ G. Lengyel, J. Appl. Phys., 37, 2 (1966) 807.

/18/ H. Fröhlich, Proc. Roy. Soc. A, 178 (1941) 493.

/19/ G. Hoyler, Siemens Forsch. and Entwickl.-Ber. 3 (1974) 110.

/20/ H. Luy, F. Oswalk, ETZ-A, 92 (1971), 358.

/21/ H. Heywang, Colloid and Polymer sci 254 (1976) 139.

/22/ J. Kammermaier, H. Hagedorn, Siemens Forsch. and Entwickl.-Ber., 2 (1973) 26.

References:

/23/ R. Behn, H. Heywant, J. Kammermaier, H. Preissinger
Siemens Z., 36 (1962) 808.

/24/ W. Vollmann, H.U. Poll, Thin Solid Films, 26 (1975) 201.

/25/ H.U. Poll, Z.angew. Physik, 29 (1970) 260.

/26/ W. Vollmann, Phys. Status Solidi (a), 22 (1974) 195.

/27/ D'Ans Lax, Taschenbuch f. Chemiker and Physiker, Vol. 1,
Berlin-Heidelberg-New York, (1967).

/28/ W. Brügel, Einführung in die Ultrarotspektroskopie,
Darmstadt, (1969).

/29/ D. Hummel, F. Scholl, Atlas der Kunststoffanalyse,
München, (1969).

/30/ L.J. Bellamy, Ultrarot-Spektrum und chemische Konstitution,
Darmstadt, (1966).

Publications:

/1/ H. Packonik
Production of thin glow-polymerized layers.
Thin Solid Films, 38,2 (1976) 171.

/2/ H. Packonik, G. Seebacher
Properties of thin glow-polymerized layers
Thin Solid Films, 38,3 (1976) 343.

OF SINAL PAGE IS
OF POOR QUALITY

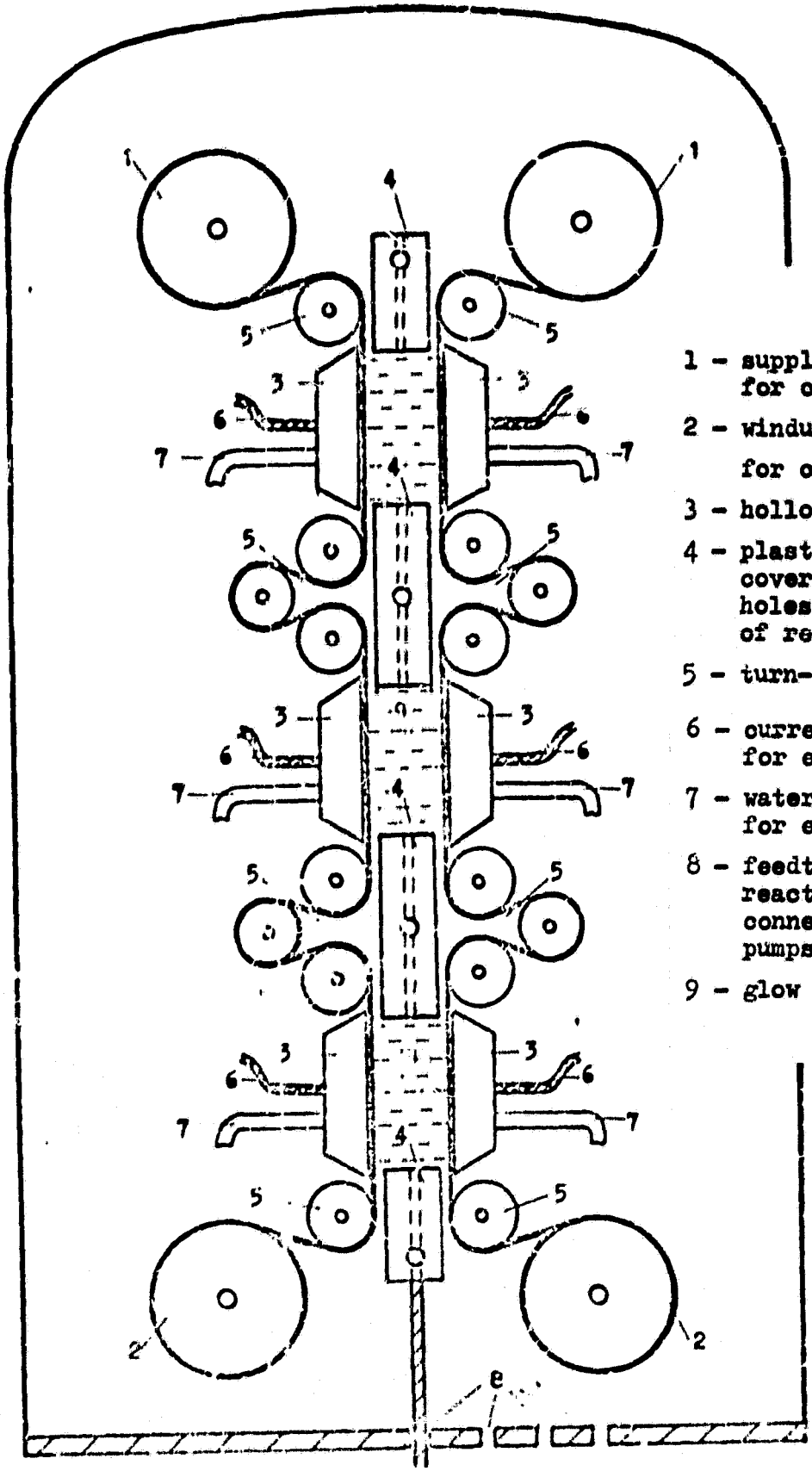

1 - supply rollers for carrier foil

2 - windup rollers for carrier foil

3 - hollow electrodes

4 - plastic electrode covers with drilled holes for supply of reaction gas

5 - turn-around rollers

6 - current supply for electrodes

7 - water connections for electrode cooling

8 - feedthroughs in reactor bottom for connections and pumps

9 - glow discharge

Figure 1: Buildup of the glow polymerization installation

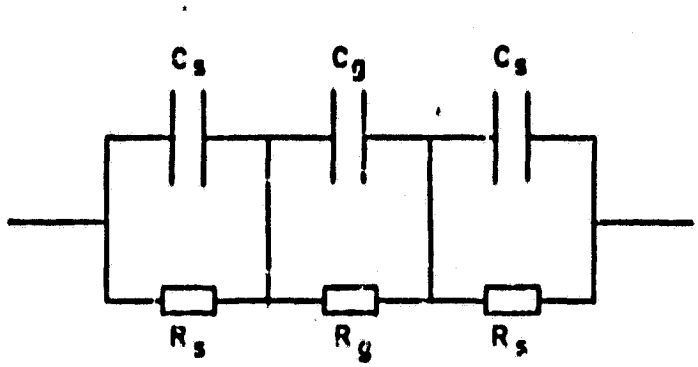

Figure 2: Substitute switch diagram of the glow discharge path

C_s capacitance of the insulation layer
C_g capacitance of the glow volume
R_s resistance of the insulation layer
R_g resistance of the glow volume

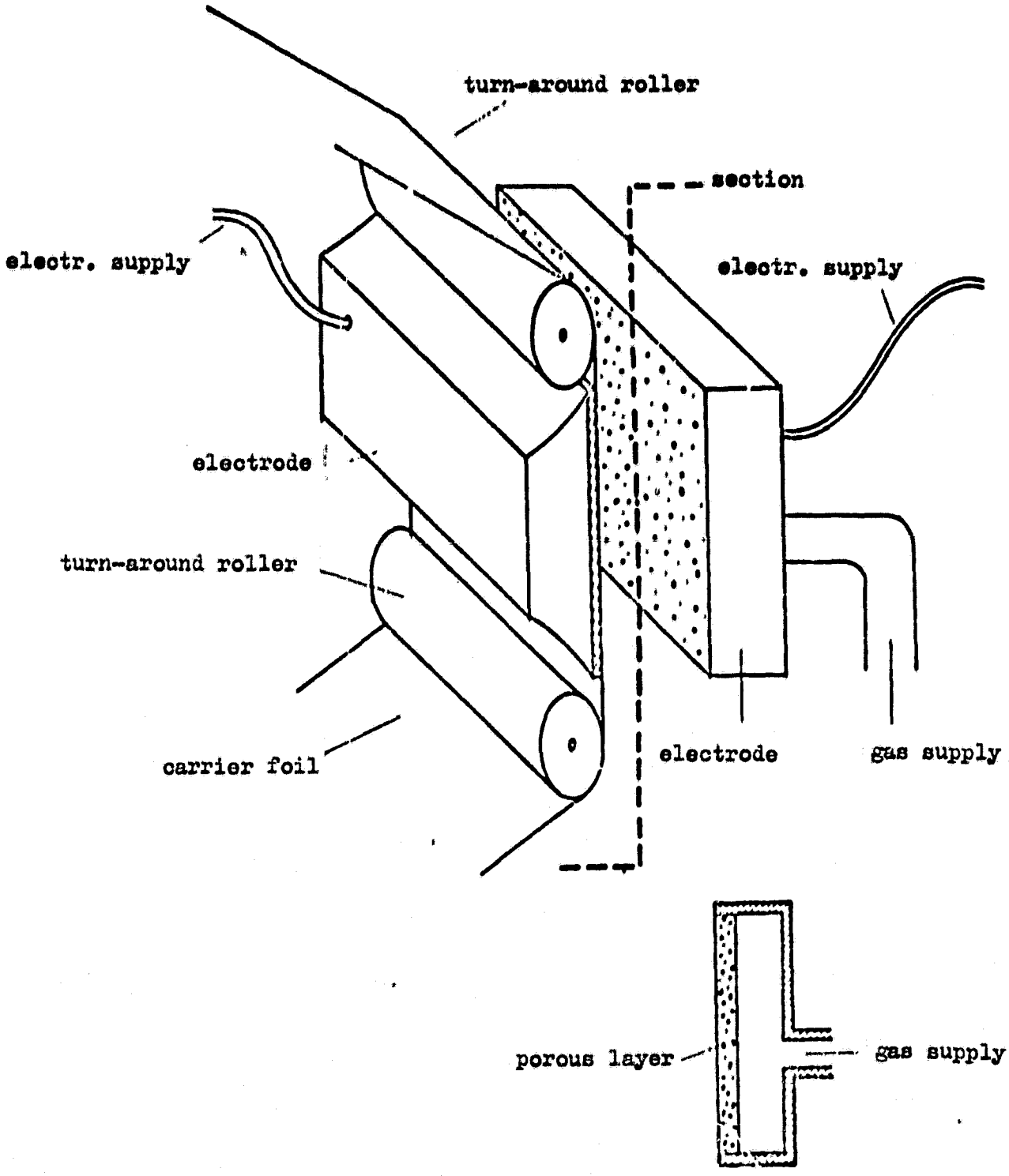

Figure 3: Buildup of the electrodes and gas supply

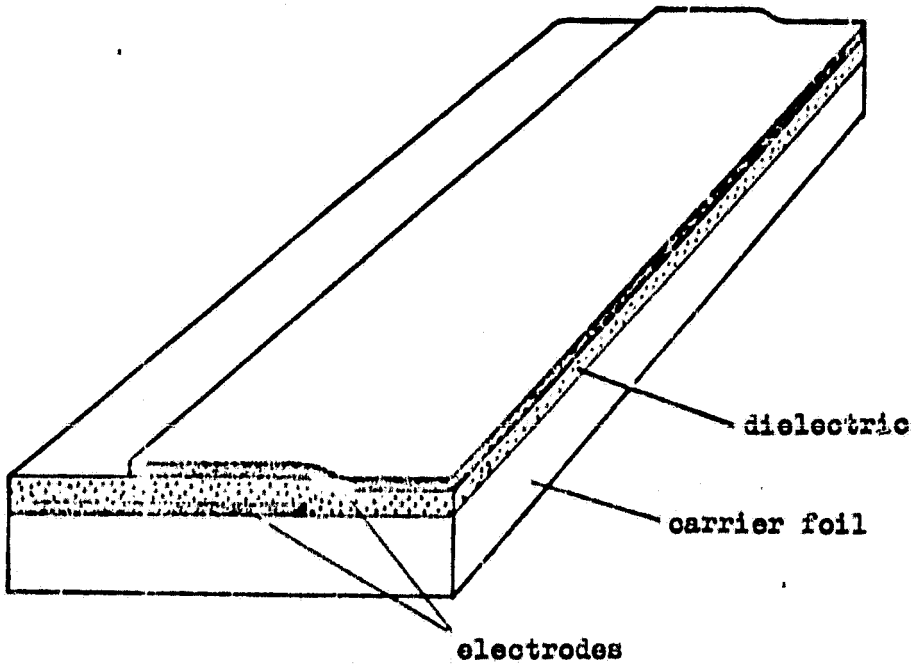

Figure 4: Buildup of the capacitor models (schematic)

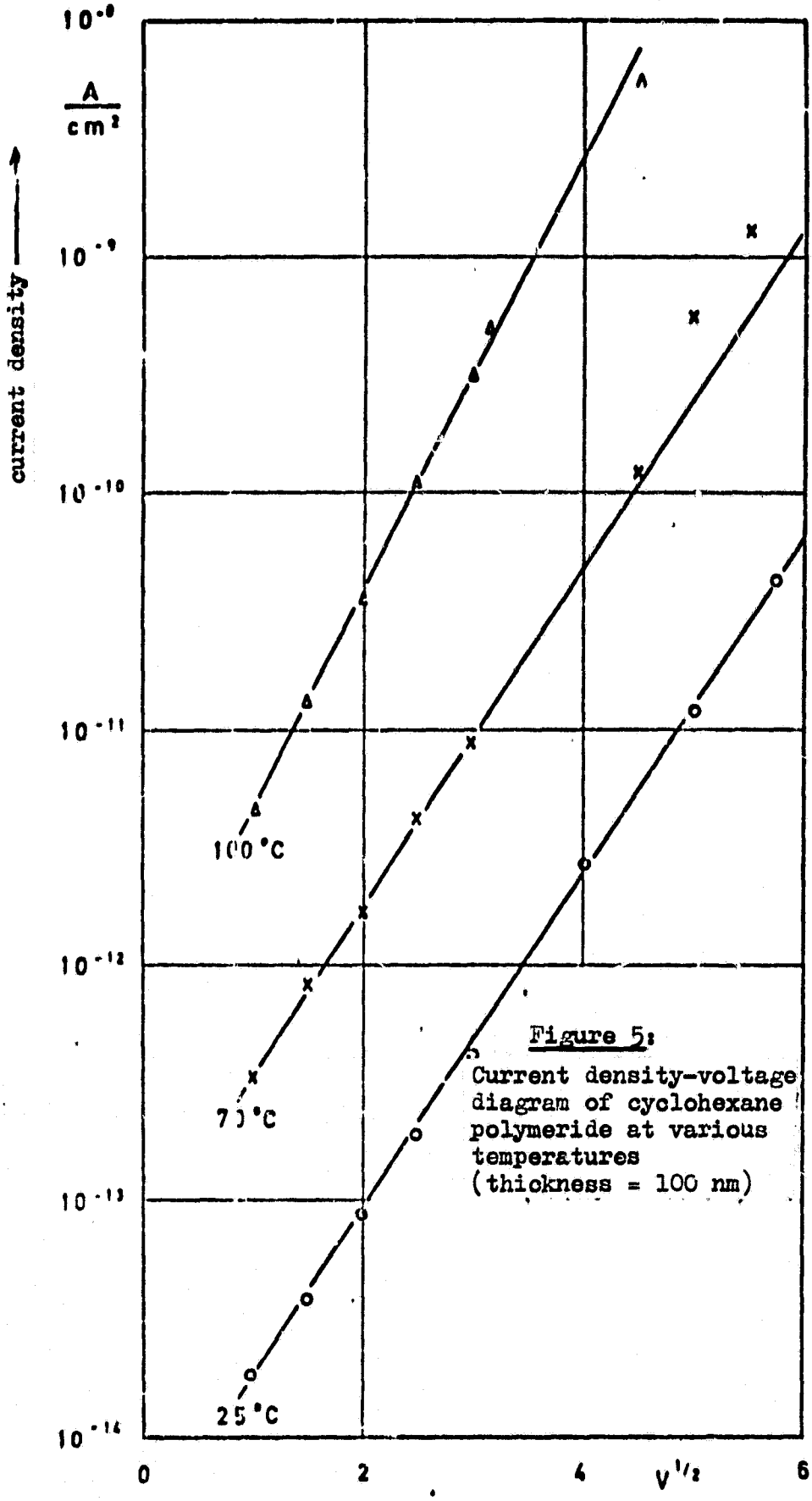

Figure 5:
Current density-voltage diagram of cyclohexane polymeride at various temperatures (thickness = 100 nm)

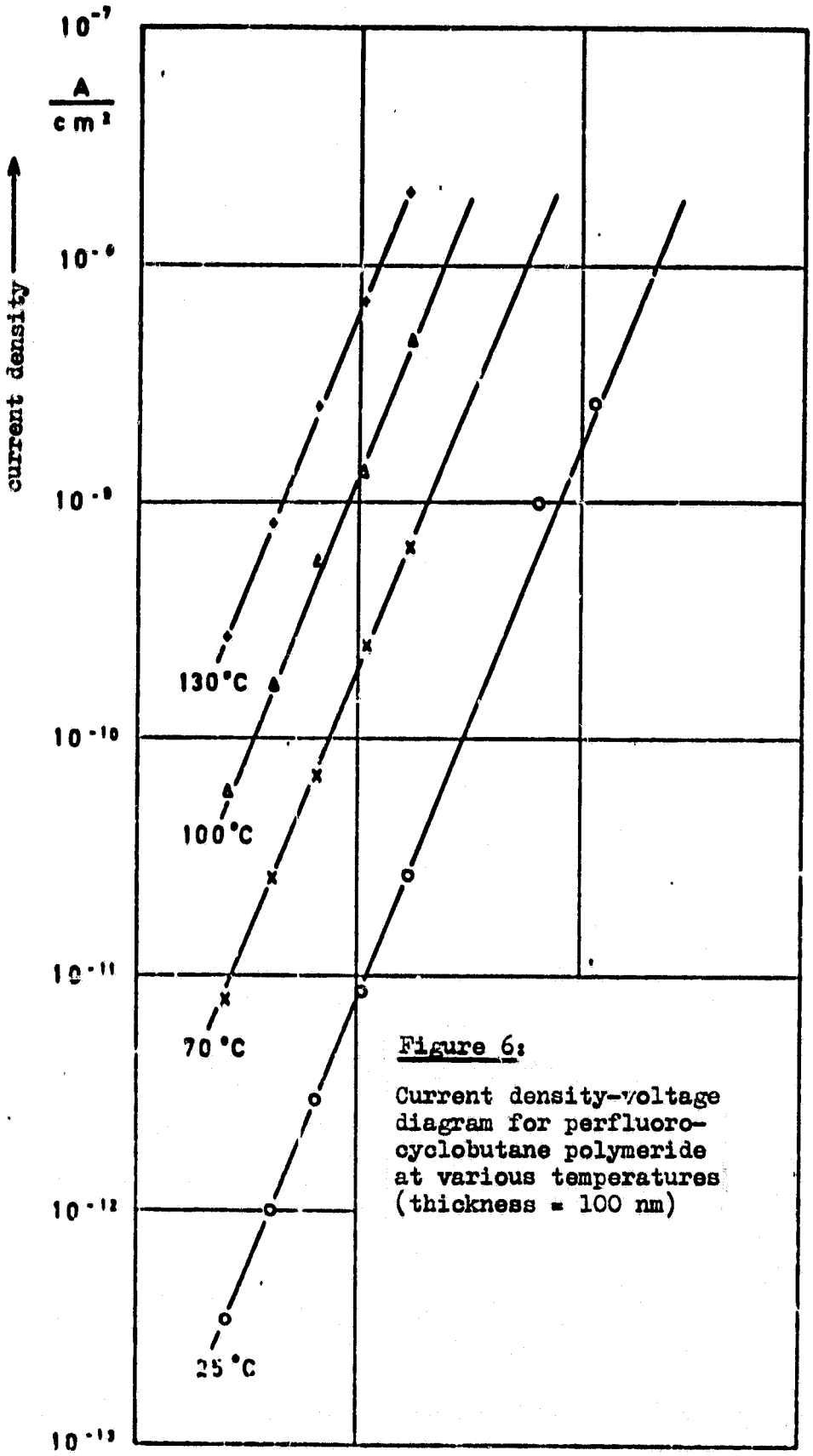

Figure 6:

Current density-voltage diagram for perfluoro-cyclobutane polymeride at various temperatures (thickness = 100 nm)

ORIGINAL PAGE IS
OF POOR QUALITY

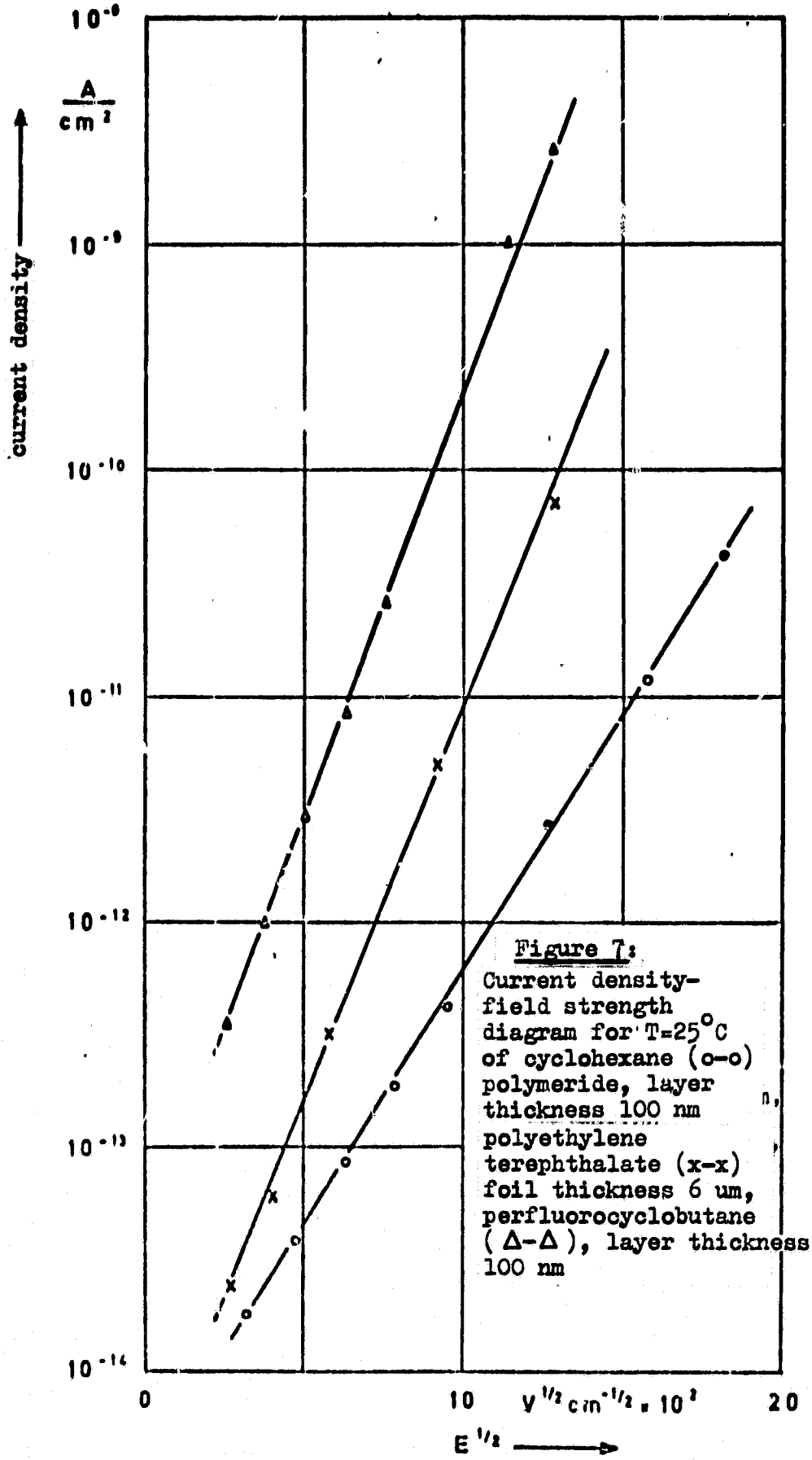

Figure 7:
Current density-field strength diagram for T=25°C of cyclohexane (o-o) polymeride, layer thickness 100 nm polyethylene terephthalate (x-x) foil thickness 6 um, perfluorocyclobutane (Δ-Δ), layer thickness 100 nm

Figure 8: Capacitance curves of densely packed glow polymer capacitors with hydrocarbon dielectric as a function of temperature

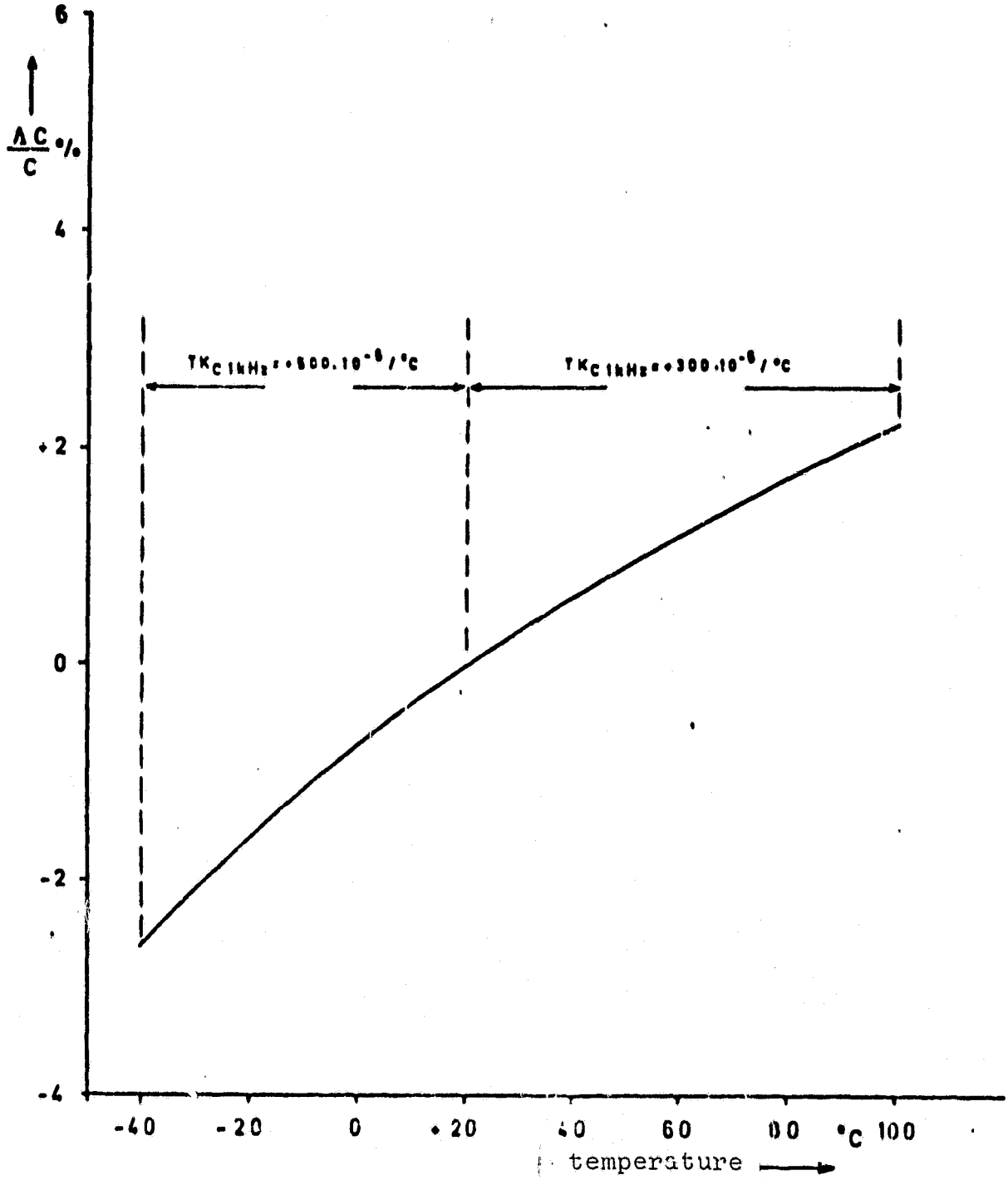

Figure 9:

Capacitance curves of densely packed glow polymer capacitors with perfluorinated dielectric as a function of temperature

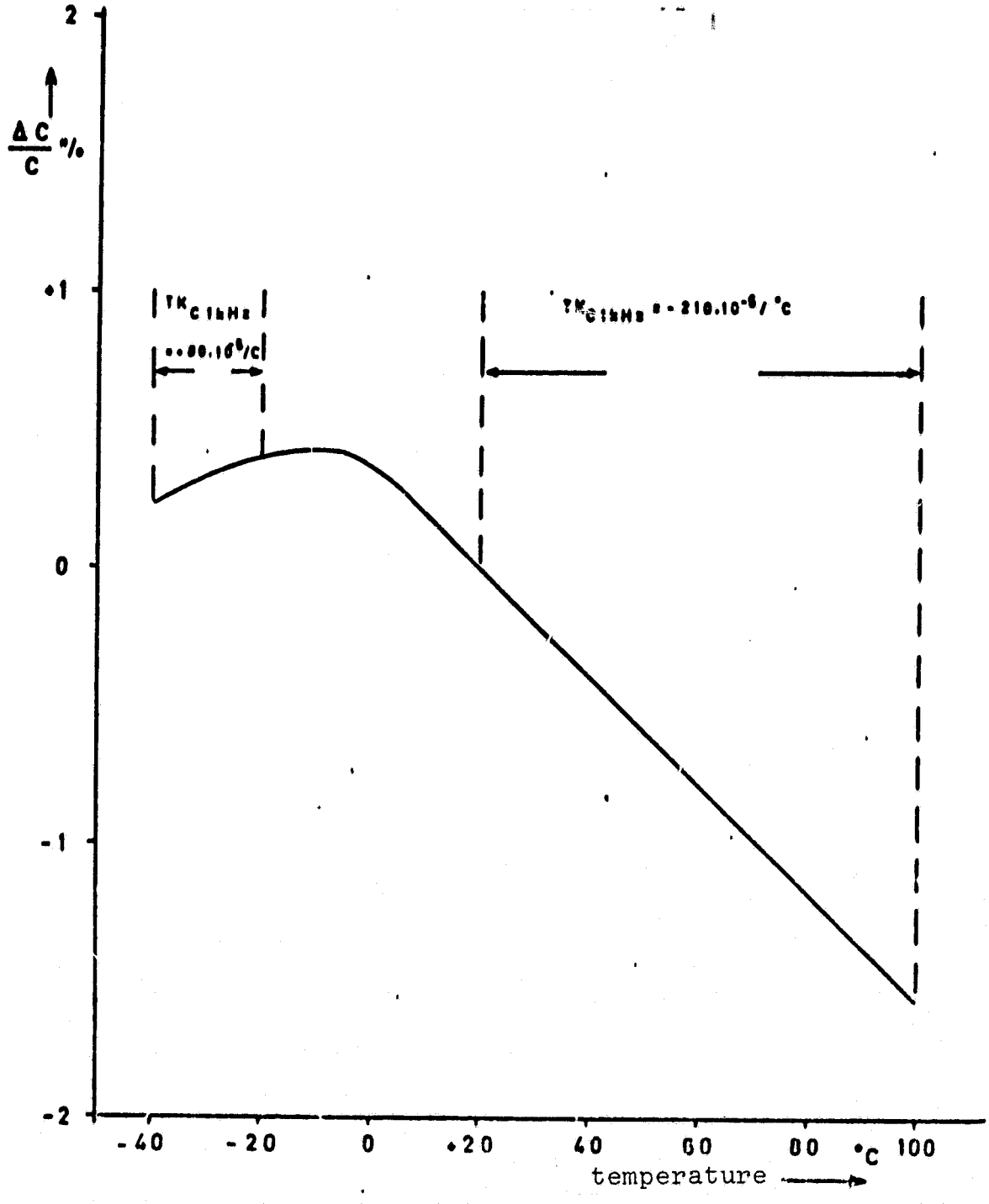

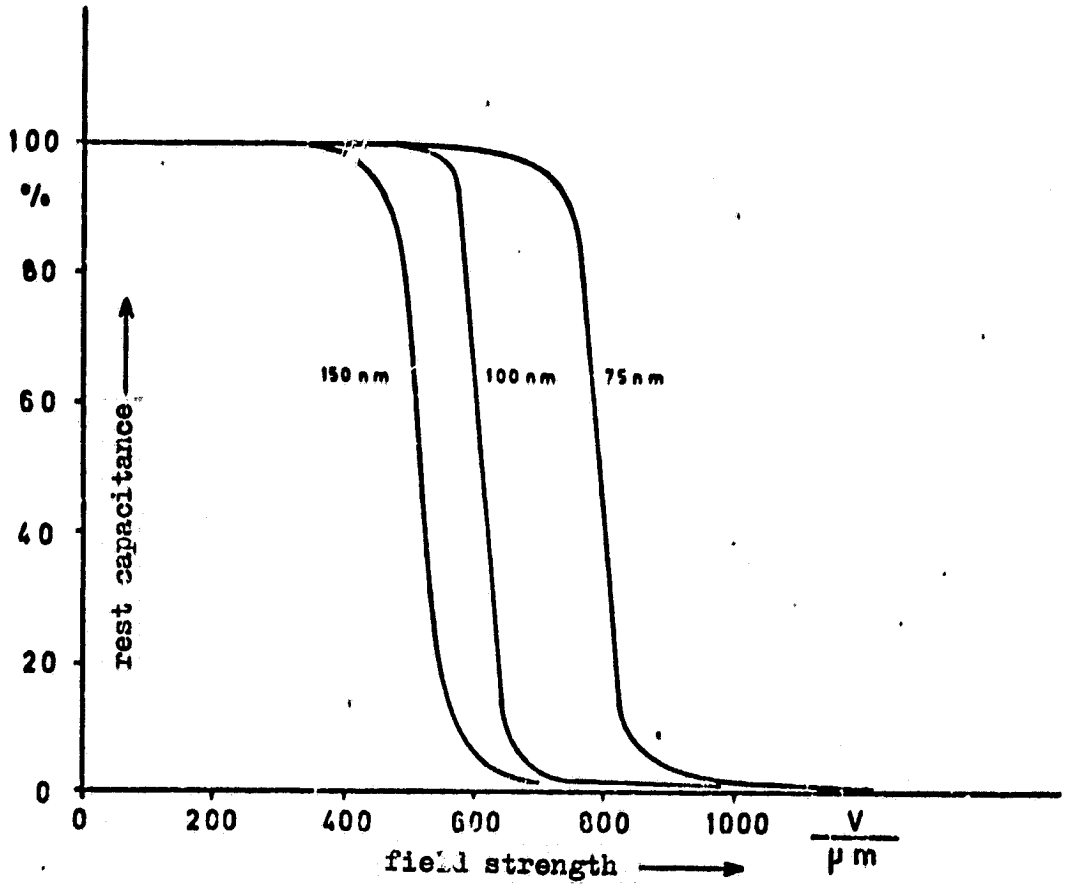

Figure 10: Capacitance decrease of condenser models with perfluorinated glow polymeride layers under voltage stresses for various dielectric thicknesses at room temperature

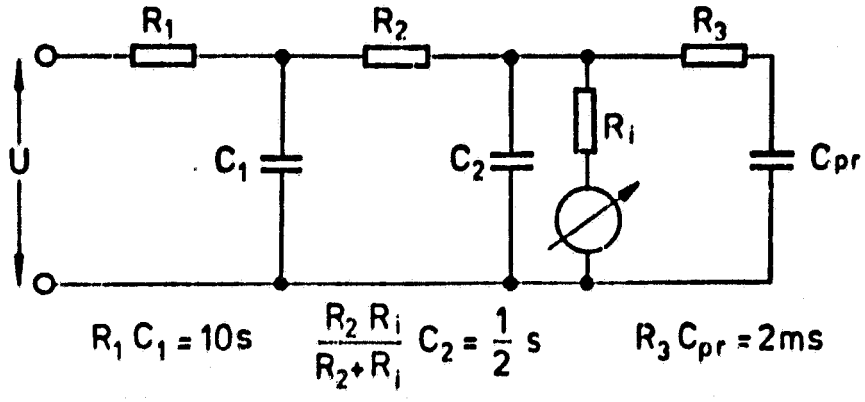

Figure 11: Measurement circuitry

C_{pr} test unit capacitance, R_i = 100 M Ω internal resistance of the oscillograph, R_1 = 1 M Ω , R_2 = 100 M Ω , R_3 = 2 M Ω , C_1 = 10 μF, C_2 = 10 nF

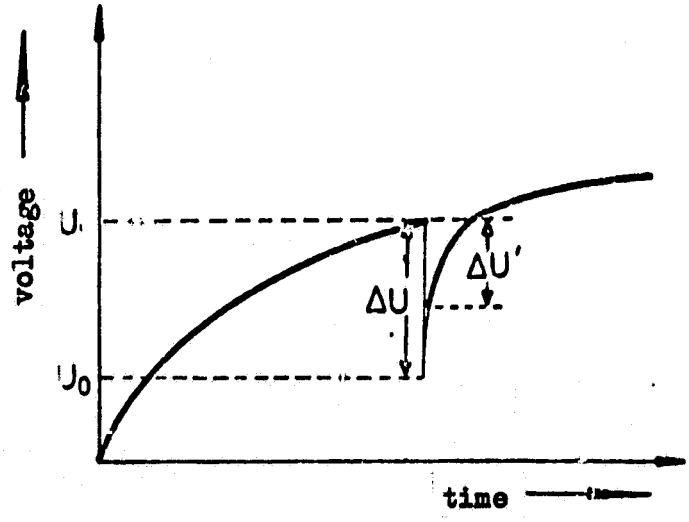

Figure 12: Voltage curve at test unit for one arcing.
Heavy solid lines represent voltage curve at C_2 recorded on the oscillogram

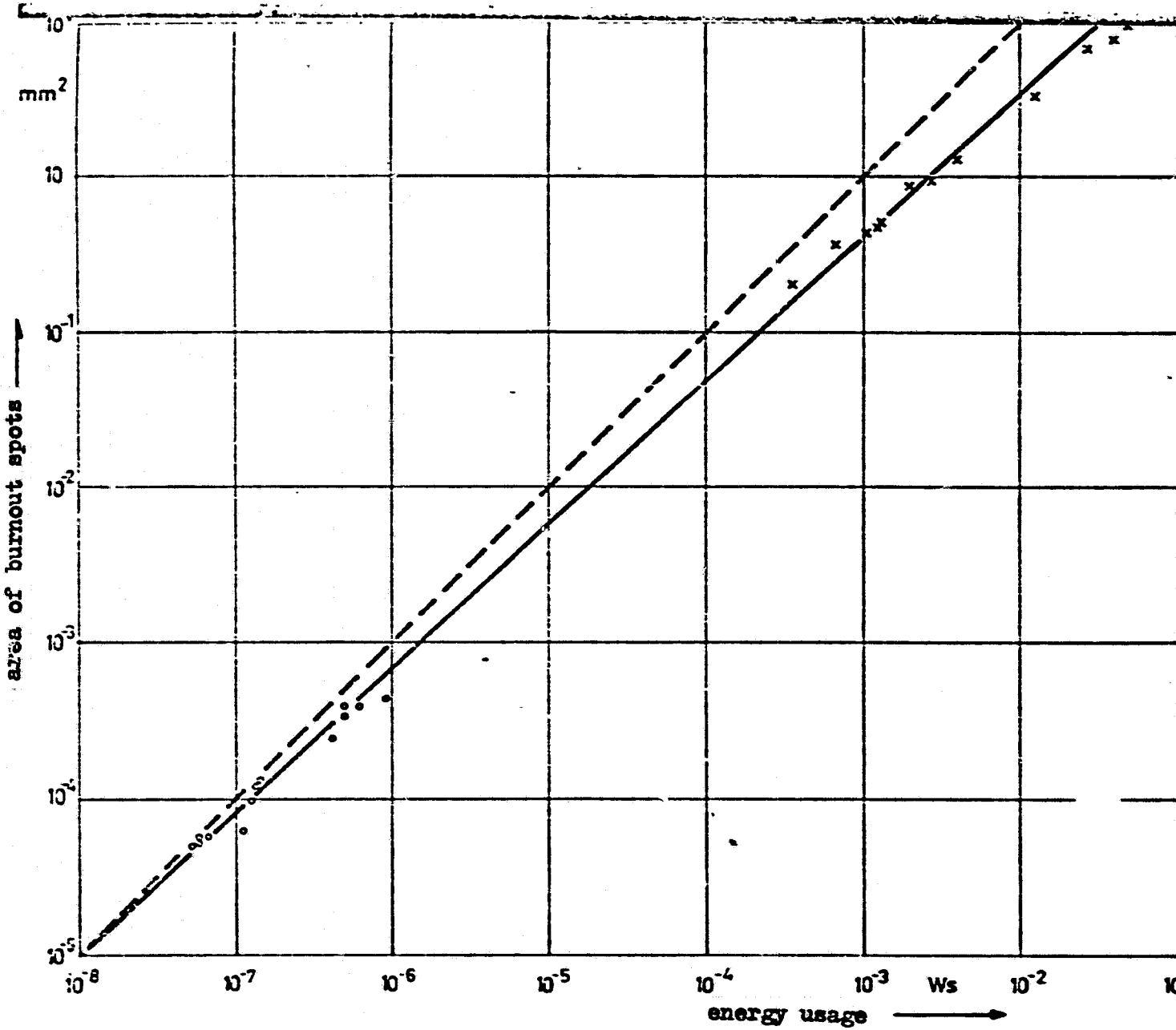

Figure 13:
Area of the burnout spots as function of energy usage

- - - energy needed for vaporizing Al-coating in the burnout spots

measured values for
x plastic foils
o glow-polymerized layers

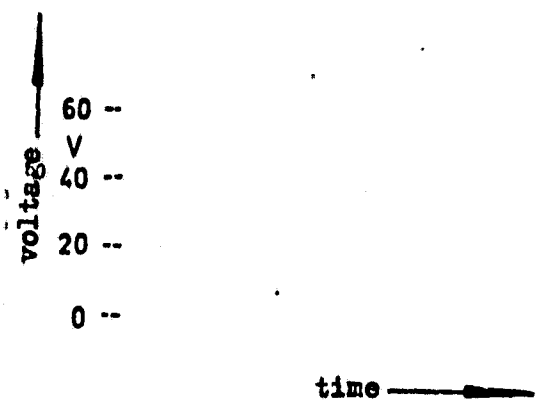

Figure 14: Arcing sequence for a series resistance of 1ΩM
Lower voltage level about equal for all arcings,
upper voltage level strongly radiated because of lower
radiation velocity

Figure 15: Energy usages, referenced to unit capacitance, of glow-polymerized capacitors as a function of arcing voltage
solid line corresponds to

$$E/C = \frac{U^2-(17V)^2}{2}$$

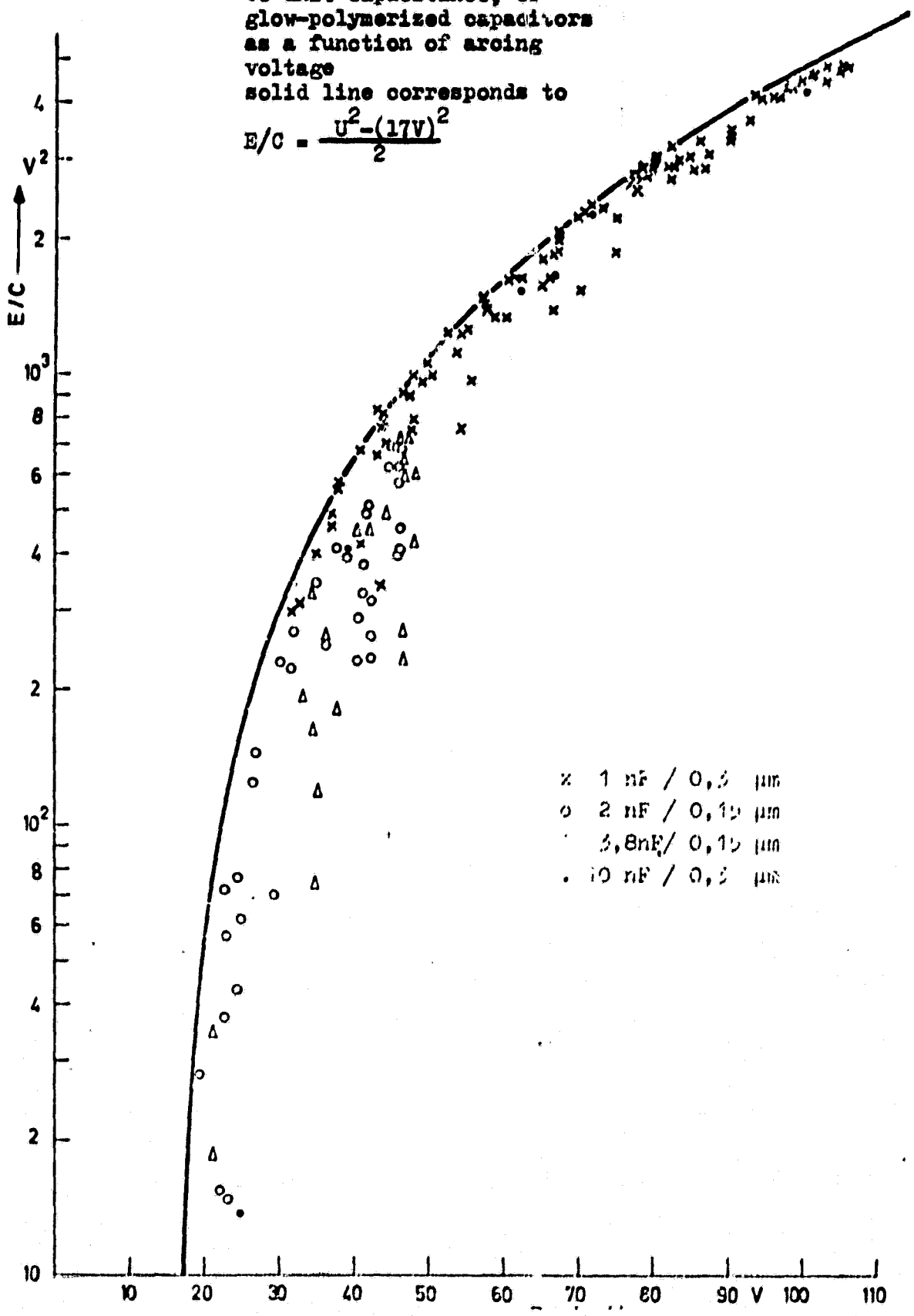

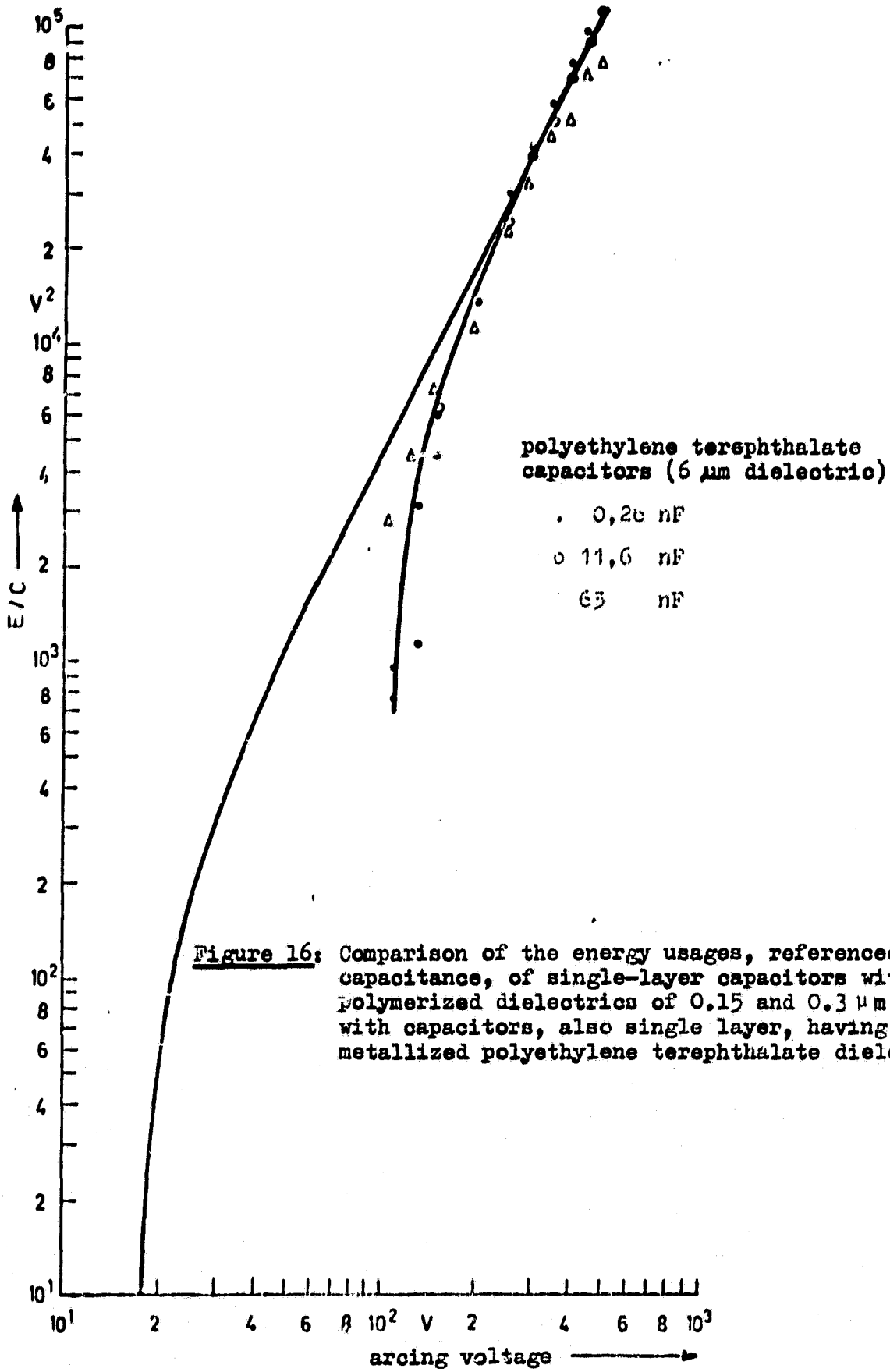

Figure 16: Comparison of the energy usages, referenced to unit capacitance, of single-layer capacitors with glow-polymerized dielectrics of 0.15 and 0.3 µm thickness with capacitors, also single layer, having 6µ µm thick metallized polyethylene terephthalate dielectrics

ORIGINAL PAGE IS
OF POOR QUALITY

Figure 17: Self-healing arcing in a glow-polymerization layer (raster-electron microscopic picture, 1000 : 1 enlargement)

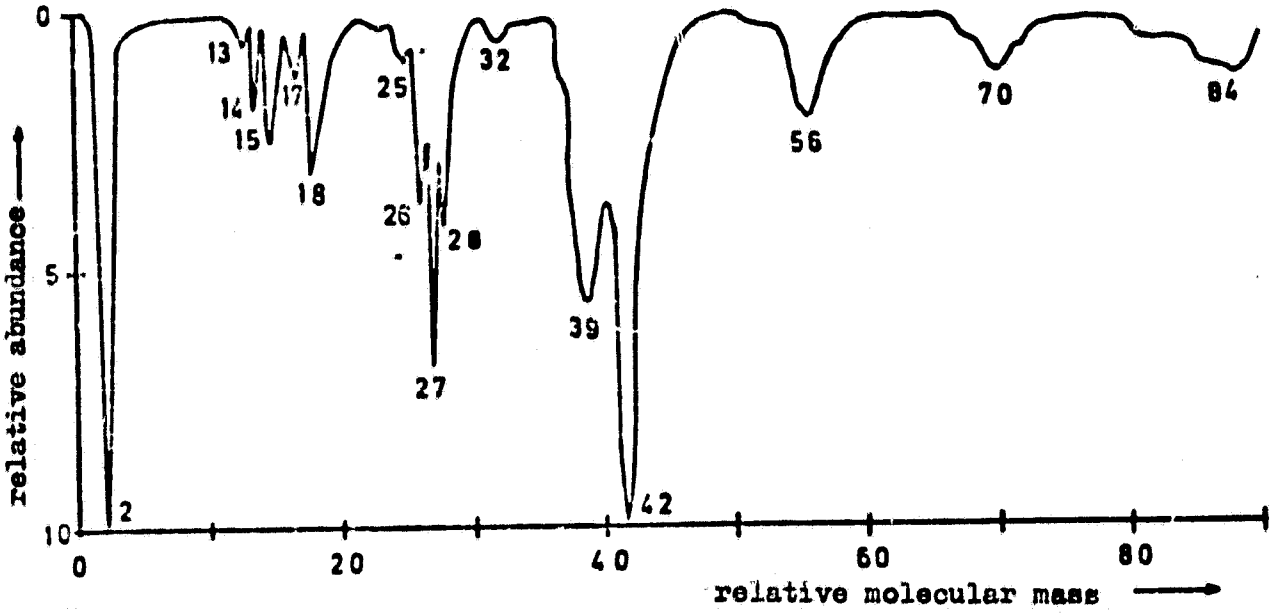

2 ≙ H_2, 13 ≙ CH, 14 ≙ CH_2, 15 ≙ CH_3, 17 ≙ OH, 18 ≙ H_2O,
25 ≙ C_2H, 26 ≙ C_2H_2, 27 ≙ C_2H_3, 28 ≙ C_2H_4, 32 ≙ O_2,
39 ≙ C_3H_3, 42 ≙ C_3H_6, 56 ≙ C_4H_8, 70 ≙ C_5H_{10}, 84 ≙ C_5H_{12}

Figure 18: Mass spectrogram of cracked products of a hydrocarbon. (assignment of the radicals to recorded relative molecular mass)

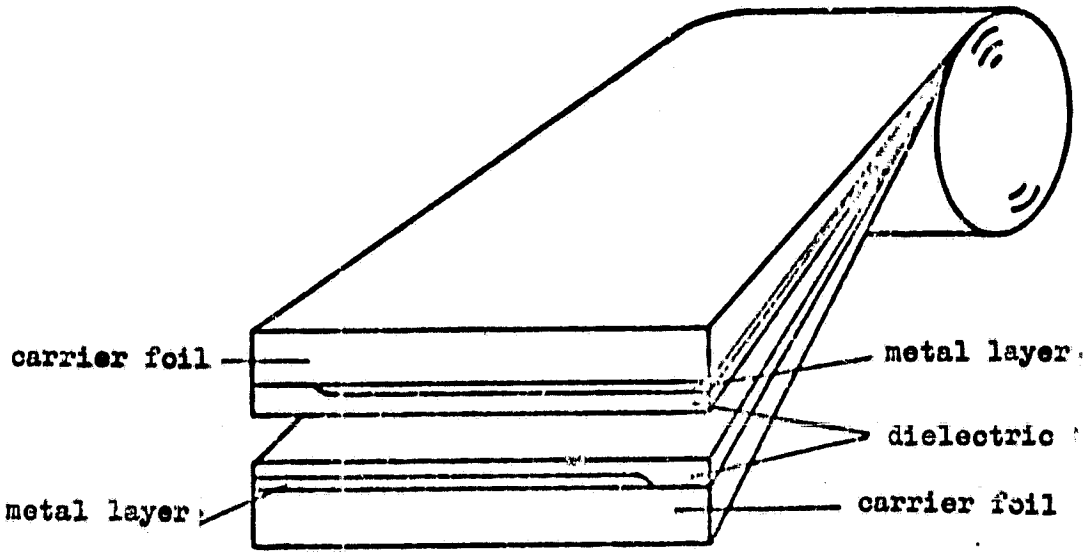

Figure 19: Buildup of a wound capacitor from two carrier foils, each having one glow-polymerization layer

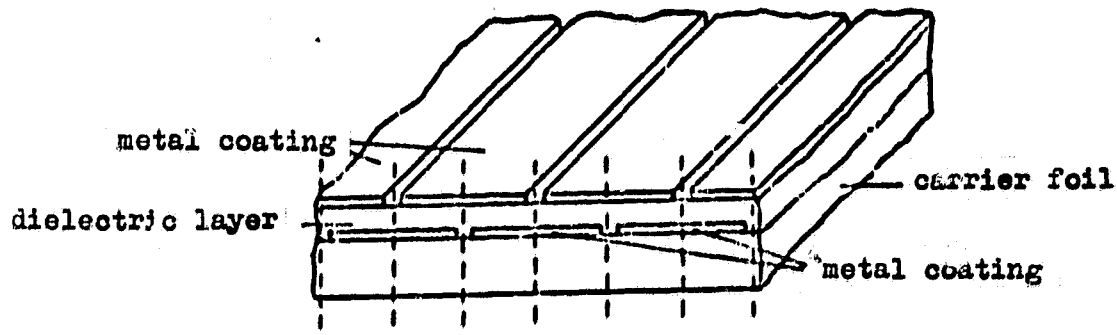

Figure 20: Sketch of a carrier foil with dielectric and metal coatings

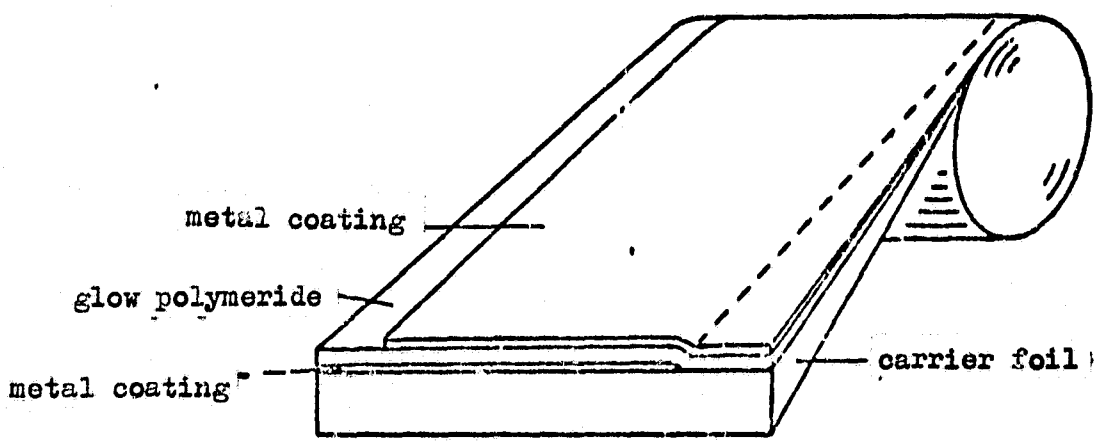

Figure 21: Buildup of a wound capacitor from a carrier foil with glow-polymerization dielectric

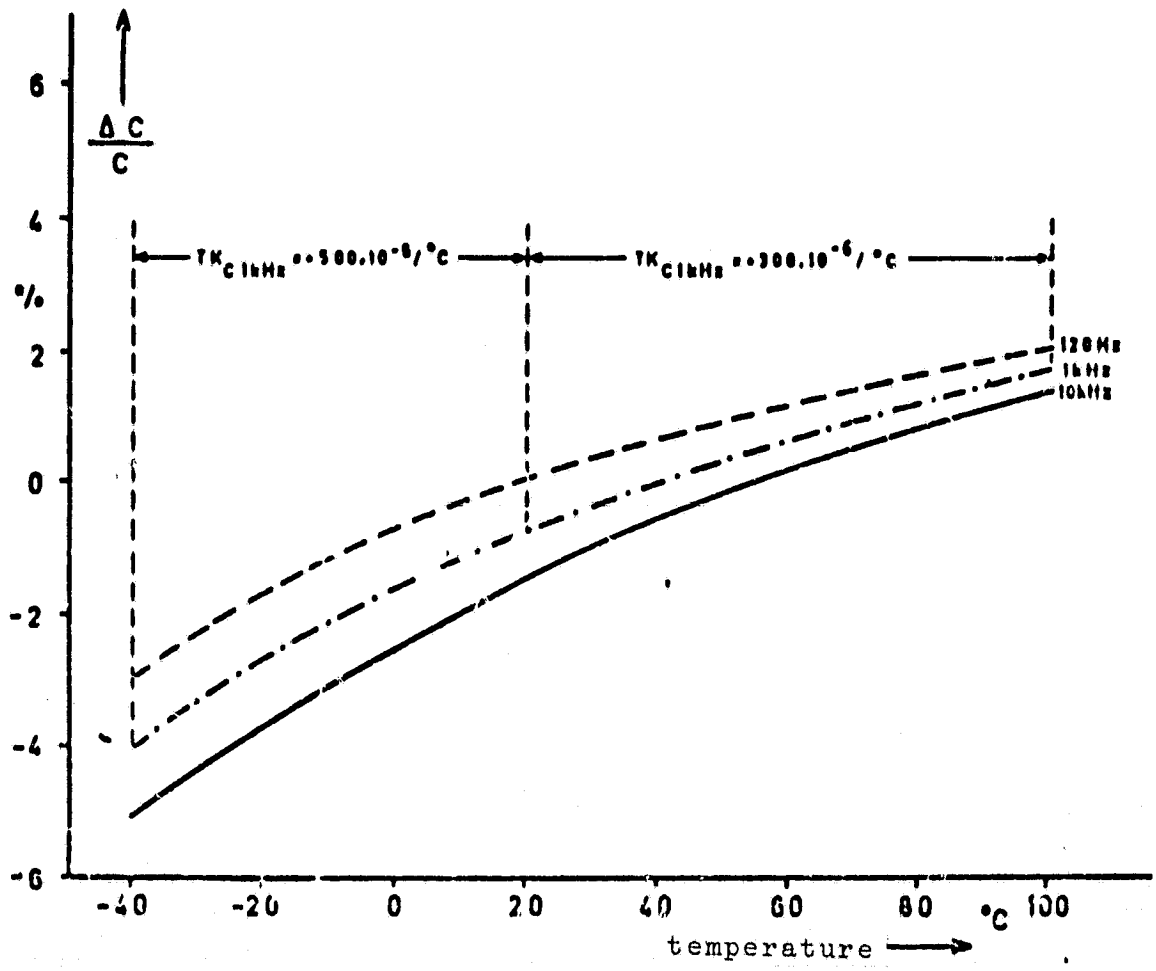

Figure 22: Capacitance curves of capacitors with a dielectric from glow-polymeride (cyclohexane 100 nm) as a function of temperature and frequency

ORIGINAL PAGE IS
OF POOR QUALITY

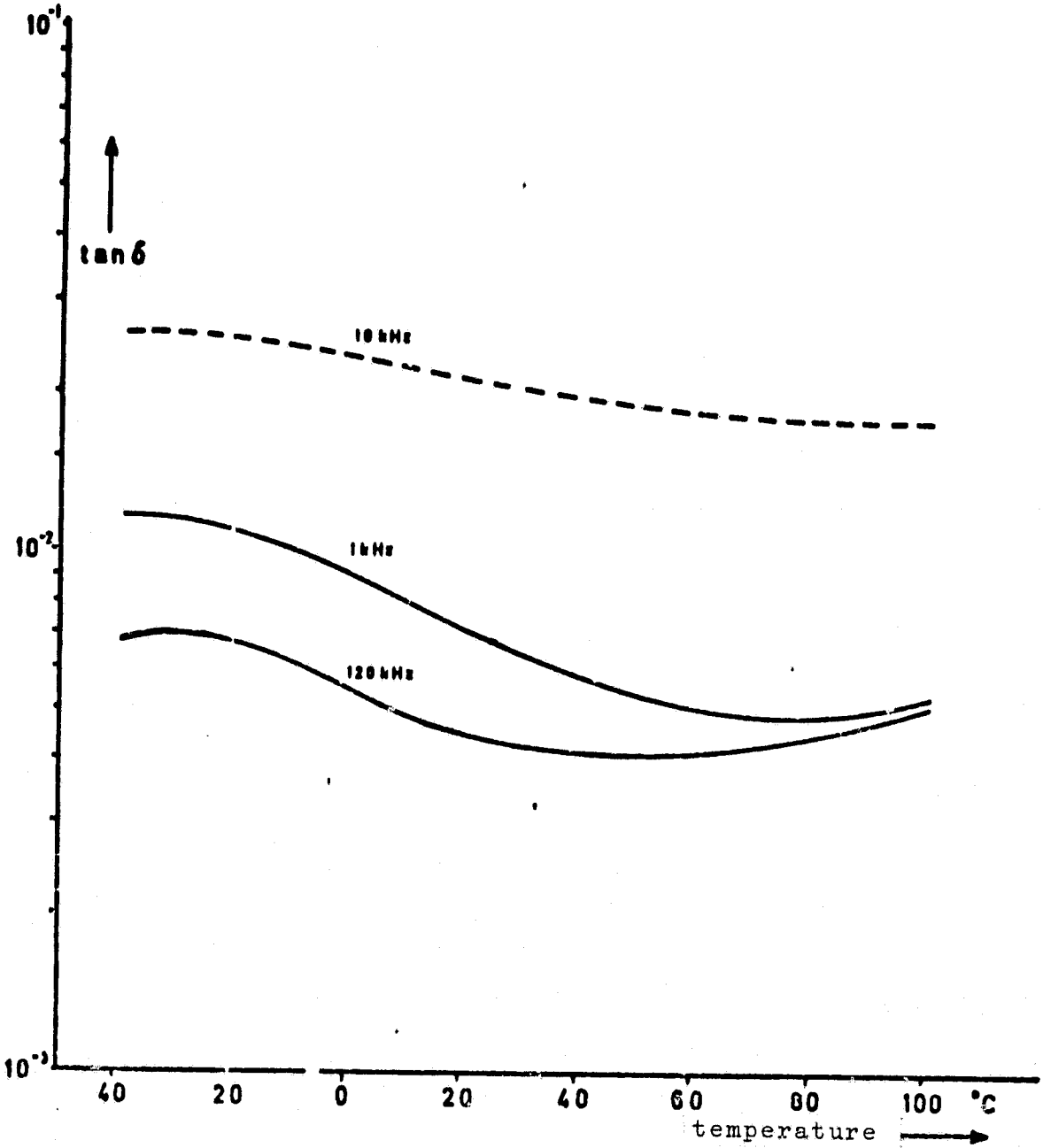

Figure 23: Loss factor curves of glow-polymerization capacitors as a function of temperature and frequency